Inorganic Chemistry
Cite This: Inorg. Chem. 2019, 58, 14507−14521
Article
pubs.acs.org/IC

Accurate Predictions of Volatile Plutonium Thermodynamic Properties

Sophie Kervazo,[†,‡] Florent Réal,[†] François Virot,[§] André Severo Pereira Gomes,[†] and Valérie Vallet*[,†]

[†]Univ. Lille, CNRS, UMR 8523-PhLAM-Physique des Lasers Atomes et Molécules, F-59000 Lille, France
[‡]Department of Chemistry and Chemical Biology, McMaster University, 1280 Main Street West, Hamilton L8S 4M1, Canada
[§]Institut de Radioprotection et de Sûreté Nucléaire (IRSN) PSN-RES, Cadarache, Saint Paul Lez Durance 13115, France

Supporting Information

ABSTRACT: The ability to predict the nature and amounts of plutonium emissions in industrial accidents, such as in solvent fires at PUREX nuclear reprocessing facilities, is a key concern of nuclear safety agencies. In accident conditions and in the presence of oxygen and water vapor, plutonium is expected to form the three major volatile species PuO_2, PuO_3, and $PuO_2(OH)_2$, for which the thermodynamic data necessary for predictions (enthalpies of formation and heat capacities) presently show either large uncertainties or are lacking. In this work we aim to alleviate such shortcomings by obtaining the aforementioned data via relativistic correlated electronic structure calculations employing the multi-state complete active space with second-order perturbation theory (MS-CASPT2) with a state-interaction RASSI spin−orbit coupling approach, which is able to describe the multireference character of the ground-state wave functions of PuO_3 and $PuO_2(OH_2)$. We benchmark this approach by comparing it to relativistic coupled cluster calculations for the ground, ionized, and excited states of PuO_2. Our results allow us to predict enthalpies of formation $\Delta_f H^{\ominus}(298.15\ \mathrm{K})$ of PuO_2, PuO_3, and $PuO_2(OH)_2$ to be -449.5 ± 8.8, -553.2 ± 27.5, and -1012.6 ± 38.1 kJ mol^{-1}, respectively, which confirm the predominance of plutonium dioxide but also reveal the existence of plutonium trioxide in the gaseous phase under oxidative conditions, though the partial pressures of PuO_3 and $PuO_2(OH)_2$ are nonetheless always rather low under a wet atmosphere. Our calculations also permit us to reassess prior results for PuO_2, establishing that the ground state of the PuO_2 molecule is mainly of $^5\Sigma_g^+$ character, as well as to confirm the experimental value for the adiabatic ionization energy of PuO_2.

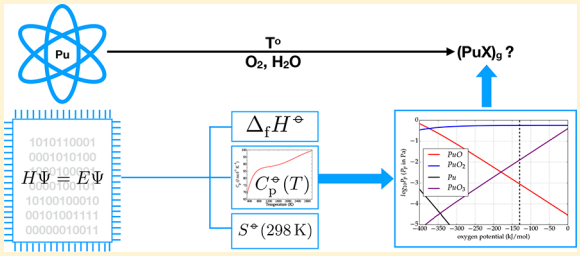

INTRODUCTION

A key step in the reprocessing of spent nuclear fuel is the PUREX (plutonium uranium refining by extraction) liquid−liquid process, through which uranium and plutonium are separated from the minor actinides. Thanks to its remarkable selectivity and the stability properties, tri-*n*-butyl phosphate (TBP) is used as the organic extractant. However, its high viscosity and density impose that the organic phase should be diluted within a hydrocarbon solvent. In the French La Hague reprocessing plant, hydrogenated tetrapropylene (HTP) is currently used as a TBP diluent. As HTP is a highly flammable substance, this could, in case of an accidental event, trigger a fire of the uranium−plutonium-containing organic solvent and may thus induce a release in the environment and atmosphere of highly radioactive species. The knowledge of their chemical behaviors is thus mandatory to carry out safety and risk analysis.

The presence of plutonium induces considerable difficulties to perform experimental investigations of solvent fires. One way to overcome these is to use a plutonium surrogate in order to carry out fire experimental campaigns. To make a selection of surrogate candidates, their behavior should be similar in all oxidation states. Considering for example the gaseous state, the volatility of Pu(VI), which still remains an open issue, should be addressed specifically because some of the candidates (Th, Ce)[1] cannot extend their oxidation degree up to VI. An alternative to surrogates is the development of a predictive model which includes all relevant physical and chemical transformations of plutonium-containing substances. Whatever the case, both approaches need reliable and accurate molecular properties of the gaseous species involved in the Pu + O + H system, required to calculate their thermodynamic properties.

The thermodynamic properties of the Pu + O + H system have been widely studied and assessed (see refs 2 and 3 and the references therein). Nonetheless, some uncertainties remain in the thermodynamic properties of some species: for the gaseous plutonium dioxide, PuO_2, the assessment of its standard heat of formation reveals a discordance between second and third law analyses of experimental data.[2] In

Received: July 13, 2019
Published: October 14, 2019

DOI: 10.1021/acs.inorgchem.9b02096
Inorg. Chem. 2019, 58, 14507−14521

Table 1. Reactions Used to Derive the Standard Enthalpies of Formation of PuO_2, PuO_3, and $PuO_2(OH)_2$

	PuO_2	PuO_3	$PuO_2(OH)_2$
R_1	$Pu + O_2 \rightarrow PuO_2$	$Pu + 3/2O_2 \rightarrow PuO_3$	$Pu + O_2 + 2H_2 \rightarrow PuO_2(OH)_2$
R_2	$Pu + 2O \rightarrow PuO_2$	$Pu + 3\,O \rightarrow PuO_3$	$Pu + 4O + 2H \rightarrow PuO_2(OH)_2$
R_3	$Pu + H_2O_2 \rightarrow PuO_2 + H_2$	$Pu + 3/2H_2O_2 \rightarrow PuO_3 + 3/2H_2O$	$Pu + 3H_2O_2 \rightarrow PuO_2(OH)_2 + 2H_2O$
R_4	$Pu + 2OH \rightarrow PuO_2 + 2H$	$Pu + 3OH \rightarrow PuO_3 + 3H$	$Pu + 4OH \rightarrow PuO_2(OH)_2 + 2H$
R_5	$Pu + 2H_2O \rightarrow PuO_2 + 2H_2$	$Pu + 3H_2O \rightarrow PuO_3 + 3H_2$	$Pu + 4H_2O \rightarrow PuO_2(OH)_2 + 2H_2$
R_6	$Pu + 2H_2O \rightarrow PuO_2 + 4H$	$Pu + 3H_2O \rightarrow PuO_3 + 6H$	$Pu + 4H_2O \rightarrow PuO_2(OH)_2 + 6H$

addition, experimental data (and in particular thermodynamic data) for other Pu(VI) molecules, such as $PuO_2(OH)_2$ and PuO_3, are scarce, and their existence in the gaseous phase remains an open question. Ronchi et al.[4] have carried out mass spectrometric measurements of effusing vapor over plutonium oxide sample where $PuO_3(g)$ has been detected but only as a nonequilibrium species. Then, transpiration experiments of plutonium oxide have been performed by Krikorian et al.[5] under oxygen as well as a mixture of oxygen and steam. From analogies with gaseous uranium species, the authors considered $PuO_2(OH)_2$ and PuO_3 molecules as the effusing species. Hübener et al.[6] have studied by thermochromatography the volatility of plutonium oxide under wet oxygen flux, and their results highlighted the formation of volatile Pu(VI) expected as $PuO_2(OH)_2$.

To predict the respective quantities of the three target volatile products of plutonium in the presence of oxygen or steam, accurate thermal functions (heat capacity, entropy, enthalpy increment) and enthalpies of formation are needed. For gas-phase molecules, this all boils down to having data on their electronic structure in order to directly calculate the vibrational−rotational partition functions. The electronic partition functions in turn require the knowledge of all the low-lying excited states within 10000 cm^{-1} and their spectroscopic labeling as degeneracies enter the statistical weights. If not known from direct spectroscopic measurements, these are often roughly estimated from chemically and spectroscopically analogous systems, such as crystals or molecules containing another actinide. However, the investigation of plutonium-containing molecules with quantum chemical methods remains a big challenge because they exhibit complex electronic structures, and as such it is often of little use to estimate their properties from chemical analogues. The presence of open 5f, 6d, and 7s orbitals on the plutonium atom leads to dense valence electronic spectra, in which the numerous degenerate or quasi-degenerate electronic states are suspected to have strong multireference characters.

A potential route for handling electron correlation and relativistic effects simultaneously for multireference heavy element complexes is to work in the four-component (4C) framework, with the Dirac−Coulomb, Dirac−Coulomb−Gaunt, or Dirac−Coulomb−Breit Hamiltonian or with the exact two-component (X2C) approaches using a molecular mean-field (MMF) approach[7] ($^2DC^M$). The multireference intermediate Hamiltonian Fock-space coupled cluster (IHFSCC) has been successfully applied to actinide-containing molecules,[8,9] though with available implementations it is not possible to treat states differing by more than two electrons from a closed-shell reference. This is problematic for PuO_3, which turns out to have a complex multireference ground state with significant contributions from configurations with two or even four unpaired electrons.[10−18] On the other hand, at the fully relativistic level, PuO_2 turns out to have a closed-shell ground state, allowing us to also estimate its standard enthalpy of formation with coupled-cluster single and double with perturbative triples ($^2DC^M$-CCSD(T)) calculations. The recent implementation of the fully relativistic EOM-CCSD method[19] offers the possibility to accurately compute the ionization potential (IP) of the PuO_2 molecule, and new arguments are proposed to clarify why the experimental values reported by Rauh et al.[20] and Capone et al.[21] differ by about 3 eV from the IP value measured by Santos et al.[22]

Considering $^2DC^M$-CCSD(T) to be the gold standard—it was shown by Shee et al.[19] that $^2DC^M$ Hamiltonian yields results which are nearly indistinguishable from the Dirac−Coulomb Hamiltonian—and the fact that there are more experimental data estimating the enthalpy of formation, the PuO_2 molecular system represents an excellent candidate to benchmark relativistic multireference methods with an a posteriori treatment of the spin−orbit coupling (SOC) interaction, namely the state-interaction-multistate second-order perturbation theory RASSI-MS-CASPT2 approach, hereafter referred to as SO-CASPT2, which has been used to compute the thermodynamic data of PuO_3 and $PuO_2(OH)_2$. High accuracy is achieved by extrapolating the electronic energies to the complete basis set limit.

The details of the calculations are described in the following section, followed by a discussion of the electronic structure of the three aforementioned molecules. We continue with an analysis of the thermodynamic properties and a comparison to available experimental data and propose new heat capacity functions and standard entropies and enthalpies of formation. Finally, the volatility of Pu(VI) species is investigated within the framework of thermodynamic equilibrium calculations. The article closes with conclusions and perspectives for nuclear safety related issues.

COMPUTATIONAL DETAILS

Chemical Reactions Used To Derive the Standard Enthalpies of Formation of PuX Molecules. To determine the enthalpies of formation, $\Delta_f H^\ominus(298.15\ K)$, of the different plutonium oxides and oxyhydroxides, we consider the reactions presented in Table 1. We begin by computing the enthalpies of the reactions presented in Table 1, as

$$\Delta_r H^\ominus = \sum_i \left(E_i + ZPE_i + [H^\ominus(298.15\ K) - H^\ominus(0\ K)]_i\right) \quad (1)$$

that is by summing up electronic energies E_i, the vibrational zero point energies (ZPE_i), and the enthalpy increment, $[H^\ominus(298.15\ K) - H^\ominus(0\ K)]_i$, at 298.15 K (see Table S1) for the products, minus that of the reactants. For a generic reaction leading to the formation of PuX ($Pu + A \rightarrow PuX + B$), the standard enthalpy of formation, $\Delta_f H^\ominus(298.15\ K)$, is computed as

$$\Delta_f H^\ominus(PuX) = \Delta_r H^\ominus - \Delta_f H^\ominus(B) \quad (2)$$

$$+\Delta_f H^\ominus(Pu) + \Delta_f H^\ominus(A) \quad (3)$$

DOI: 10.1021/acs.inorgchem.9b02096
Inorg. Chem. 2019, 58, 14507−14521

using the known enthalpies of formations of the Pu and A reactants and the B product listed with their uncertainties in Table S1 of the Supporting Information.[23,24] Note that, because of the lack of thermodynamics data on plutonium species, it is not possible to use reactions that are isogyric or isodesmic, which might alter the final accuracy of our results; the measure of the resulting uncertainties within the 95% confidence limit obtained for the average of these reactions is computed as explained in the Supporting Information and reported in Table 9.

Two-Step Relativistic Calculations. *Geometries and Enthalpy Corrections.* The geometries were obtained from scalar relativistic DFT calculations, except for PuO_2, for which the optimal $^2DC^M$-CCSD(T) geometry was used. In the DFT calculations, the plutonium atom was described by a relativistic effective core potential (RECP) ECP60MWB[25] with the corresponding basis set of quadruple-ζ quality,[26] while for the lighter atoms augmented triple-ζ (aug-cc-pVTZ)[27] basis sets were used. All of the DFT calculations were carried out with the B3LYP functional[28] and the GAUSSIAN09[29] package. The ZPE values and enthalpy corrections needed in eq 1 were calculated from the harmonic vibrational frequencies. Anharmonic corrections to the vibrational partition functions were not included, as these would contribute only a few tenths of a kJ mol^{-1} at most and only or those species involving hydrogen atoms. Using the vibrational perturbation theory[30,31] as implemented in Gaussian,[29] we have computed the anharmonic corrections for all molecules. The largest contribution to any of the reaction enthalpies was only 5 kJ mol^{-1}, even at temperatures as high as 3000 K, which is considered negligible for the accuracy goal of the present work.

Basis Sets and Extrapolation to the Complete Basis Set Limit. To reach high accuracy for ab initio thermochemistry, the computed electronic energies were extrapolated to the complete basis set limit (CBS), from two calculations with all-electron atomic natural orbitals relativistic core correlation (ANO-RCC) basis sets[32,33] with quality sequentially increased from triple-ζ (n = 3) to quadruple-ζ (n = 4). The CASSCF/HF energies were extrapolated with the Karton and Martin formula[34]

$$E_n^{\mathrm{CAS/HF}} = E_{\mathrm{CBS}}^{\mathrm{CAS/HF}} + A(n+1)\exp(-6.57\sqrt{n}) \quad (4)$$

separately from the correlation energies E_n^{corr} via[35,36]

$$E_n^{\mathrm{corr}} = E_{\mathrm{CBS}}^{\mathrm{corr}} + \frac{B}{(n+1/2)^4} \quad (5)$$

While irregular basis convergence patterns was reported for lanthanide ANO-RCC basis sets,[37] the convergence is smooth in the case of the Pu basis sets, as illustrated by Figure S1 in the Supporting Information.

Single-Reference Wave Function Correlated Calculations. To account for dynamic electronic correlation, in cases of open-shell systems with a weak multireference character, UCCSD(T) (unrestricted coupled cluster singles doubles and perturbative triples)[38] is the gold standard. These calculations were performed using the Molpro Quantum Chemistry software.[39] The frozen orbitals were the 1s orbital of O and 1s to 5d (included) orbitals of Pu. Core−valence correlation effects were discarded not only due to their high computational cost but also because we expect them to be no larger than 4 kJ mol^{-1} for actinide molecules.[40,41] Due to the important multiconfigurational character of the ground-state wave function of PuO_3 and $PuO_2(OH_2)$ species, no UCCSD(T) calculations were performed.

Multireference Calculations and Definition of the Orbital Active Spaces. Knowing the multiconfigurational character of the ground-state wave function of the atomic plutonium and the plutonium oxides and oxyhydroxides of interest,[10] and since SOC needs to be included *a posteriori*,[42] the use of a multiconfigurational approach that accounts for the static and dynamic electronic correlation effects is mandatory. The former was included with the CASSCF (Complete Active Space Self Consistent Field) method.[43,44] The active spaces are listed in the Table 2; for the atoms (O, H, Pu) and molecules without Pu (OH, H_2O_2, H_2, H_2O), the active space is composed of the valence orbitals.

Table 2. Active Spaces for the Various Plutonium Oxides and Oxyhydroxides

molecule	active space (electron, orbitals)	orbitals
PuO_2	(4,4)[a]	$\delta_u(2)$, $\phi_u(2)$
PuO_2	(12,17)[b]	$\pi_u(2)$, $\pi_g(2)$, σ_g, σ_u, $\pi_u^*(2)$, $\pi_g^*(2)$, σ_g^*, σ_u^*, $\delta_u(2)$, $\phi_u(2)$, $\delta_g(2)$
PuO_3	(14,13)[c]	$1a_1$, $2a_1/\pi_u$, $2a_1$, $4a_1/p_x^O$, $5a_1/\phi_u$, $6a_1/\pi_u$, $1b_1/\phi_u$, $2b_1/\pi_u$, $1b_2/p_z^O$, $2b_2/\sigma_u$, $3b_2/\delta_u$, $4b_2/\sigma_u^*$, $1a_2/\delta_u$
$PuO_2(OH)_2$	(4,4)	$1a/\delta$, $2a/\phi$, $1b/\delta$, $2b/\phi$
Pu	(8,13)	7s, 5f, 6d
O	(6,4)	$2s$, $2p_x$, $2p_y$, $2p_z$
O_2	(12, 8)	σ_{2s}, σ_{2s}^*, σ_{2p}, σ_{2p}^*, $\pi_{2p}(2)$,$\pi_{2p}^*(2)$
OH	(7,5)	σ, σ_{nb}, $2p_x^O$, $2p_y^O$, σ^*,
H_2O_2	(14, 10)	1 σ^{O-O}, 1 σ^{*O-O}, $\sigma^{O-H}(2)$, 2 σ^{O-O}, π^{O-O}, $2p^O$, $1\sigma^{*O-O}$, $\sigma^{O-H}(2)$
H_2O	(8,6)	$2a_1$, $1b_2$, $3a_1$, $1b_1$, $4a_1$, $1b_2$
H_2	(2, 2)	σ_g, σ_u^*
H	(1,1)	1s

[a]For the ground-state energy calculation. [b]For ground and excited states that are coupled by the spin−orbit Hamiltonian in the RASSI. [c]The orbital numbering refers to the active space: e.g., $1a_1$ is the first active orbital of a_1 symmetry.

Nevertheless, one has to note that the CAS (Complete Active Space) of (8,13) for the plutonium atom lead to convergence problems as the competing configurations $5f^67s^2$, $5f^66d^17s^1$, $5f^66d^17s^27p^1$ are close in energy and intertwined.[45−47] We instead used a RAS (Restricted Active Space)[48] to focus on the two configurations $5f^67s^2$, $5f^6d^17s^1$ that dominate the low-lying part of the Pu spectrum (up to 18 000 cm^{-1}. The RAS space includes the 7s in the RAS1, the 5f in the RAS2 and the 6d in RAS3 with one as the maximum number of holes in RAS1 and as number of particles in RAS3.

For the plutonium molecules, the difficulty is to design orbital active spaces that do not exceed the current active space limit of about 16 electrons in 16 orbitals. In a recent work, some of us have used the multireference density matrix renormalization group (DMRG) calculations,[10] in which we could afford including all the valence orbitals from both Pu and oxygen atoms into the active space, thus allowing the maximum flexibility into the ground-state wave functions. These DMRG calculations cannot be used for quantitative thermodynamics calculations, as they were restricted to a DMRG-CI approach and did not include orbital relaxation, dynamic correlation, and SOC. However, concepts of quantum information theory, such as orbital-pair correlations, were helpful to identify which orbitals contribute most to the ground-state wave functions, helping the design of reduced "optimal" active spaces[10] that can be reasonably handled in the SO-CASPT2 calculations carried out here.

Regarding PuO_2 (symmetry D_{2h}), the choice of the active space to describe the low-lying excited states was based on the work of Denning et al.[49] and La Macchia et al.[50] The full valence active space is composed of 2 π_u, 2 π_g, σ_g, and σ_u bonding orbitals, which are combinations of 5f and 6d orbitals of plutonium mixed with the 2p orbitals of the oxygen atoms, the corresponding antibonding orbitals, and the four nonbonding δ_u, ϕ_u.

Despite the increase of the computational power, a CASSCF calculation with the full valence active space[10] made of 16 electrons in 19 orbitals is still not feasible (203440360 CSF for the $^5\Sigma_g^+$ ground state). We thus chose to remove the two lowest doubly occupied π_g orbitals, leading to an active space of 12 electrons in 17 orbitals. Note that La Macchia et al.[50] used a smaller active space of 12 electrons in 14 orbitals, as they discarded the π_g^* and σ_g^* antibonding orbitals. Whereas for a good estimate of SOC effect in a two-step approach, numerous excited states have to be computed (to position accurately the excited states with respect to the ground state), this could degrade the description of the ground state in terms of total energy and wave

DOI: 10.1021/acs.inorgchem.9b02096
Inorg. Chem. 2019, 58, 14507−14521

function.[51] Thus the ground-state $^5\Sigma_g^+$ spin-free energy is computed from the well-suited minimal active space that distributes four electrons in the four nonbonding orbitals (δ_u and ϕ_u), denoted SO-CASPT2(4,4).

To define the important orbitals in the active space of PuO_3 (symmetry C_{2v}), we used information from PuO_2^{2+} that can be considered as a subunit of plutonium trioxide suggesting an active space composed of two π orbitals, one σ orbital along with the corresponding antibonding associated to the plutonyl PuO_2^{2+} subunit, the four nonbonding δ_u and ϕ_u orbitals, and the p_x, p_y, and p_z of the third distant oxygen; this sums up to an active space of 14 electrons distributed in 13 orbitals as depicted in ref 10. The active space to treat the cationic form PuO_3^+ includes one electron less.

For $PuO_2(OH)_2$ (symmetry C_2), the strengths of the orbital-pair correlations depicted in ref 10 indicate that the nonbonding δ_u and ϕ_u orbitals of Pu are the most entangled orbitals and should be part of a chemically relevant active space for the ground-state wave function as well as the low-lying excited states. This yielded 16 electronic excited spin-free states. For the other Pu systems, it was not possible to include all states. Indeed, the higher excited states turned out to have too low reference weights (<20%) in the multi-state complete active space with second-order perturbation theory (MS-CASPT2)[52] wave functions.

The case of the Pu atom was peculiar, since the RASSCF was not able to reproduce the exact degeneracy of the states of the same L value. Therefore, the degeneracy was manually imposed across states with identical L and S values. The CASSCF and MS-CASPT2 calculations finally include 80, 119, and 16 electronic states for PuO_2, PuO_3, and $PuO_2(OH)_2$, respectively as detailed in Table S6 in the Supporting Information. For the UCCSD(T) calculations the 1s orbital of O and the 1s to 5d orbitals (included) for Pu were kept frozen. To guarantee a good description of all the states, an imaginary shift of 0.05 au[53] was added to the zeroth-order Hamiltonian in addition to the IPEA = 0.25 au correction.[54]

Spin–Orbit Coupling State Interaction Method. For the Pu atom and the plutonium molecules, SOC was treated a posteriori by state interactions between the MS-CASPT2 wave functions, using the restricted active space state interaction (RASSI) program,[55] with spin–orbit integrals computed in the atomic mean field approximation using the AMFI code.[56,57] These results are referred to as SO-CASPT2. The SOC contributions to the ground-state energies, i.e. the difference between the ground-state spin-free MS-CASPT2 energies (SF-CASPT2) and the SO-CASPT2 energies, was added to all other scalar relativistic results, such as the DFT and UCCSD(T) results. In Table 9, ΔE_{SO} corresponds to the difference between the SOC contributions of the plutonium molecule and the atomic Pu. All SO-CASPT2 calculations were performed with the MOLCAS8 package.[58]

One-Step Relativistic Correlated Calculations. We also performed one-step relativistic calculations based on the molecular mean-field[7] approximation to the Dirac–Coulomb ($^2DC^M$) Hamiltonian, at MP2, CCSD, and CCSD(T)[59,60] levels of theory with DIRAC18 electronic structure code[61] for Pu, PuO_2, H_2, OH, H_2O, and H_2O_2. This allowed us to obtain the energies for reactions R_3–R_6 yielding PuO_2.

The Dyall basis sets[62,63] of triple- and quadruple-ζ quality were employed for the plutonium atom and Dunning's aug-cc-pVnZ (n = 3, 4) sets[27] for the light elements, all of which are left uncontracted. These calculations have been performed in $D_{\infty h}$ symmetry for Pu, PuO_2, and H_2, in $C_{\infty v}$ symmetry for OH, in C_{2v} symmetry for H_2O, and in C_1 symmetry for H_2O_2. In all cases, we've employed the approximation of the (SS|SS)-type two-electron integrals by a point-charge model.[64] Electrons in molecular spinors with energies between −3 and 100 au were included in the correlated treatment, which amounted to correlating 28 electrons for PuO_2, 16 for Pu, 12 for H_2O_2, 6 for OH and H_2O, and 2 for H_2.

For PuO_2, the SCF calculations were closed-shell ones, with 52 and 58 electrons in g and u irreducible representations, respectively. For this species, the equilibrium structure and stretching frequencies were determined via a polynomial fit of the potential energy surface constructed from single-point calculations for symmetric and antisymmetric Pu–O stretching modes. Because of constraints in computational resources, the O–Pu–O bending mode frequency was obtained from $^2DC^M$-CCSD(T) calculations correlating a smaller number of spinors between −3 and 5 au. Energies and potential energy curves at the complete basis set limit were obtained with the same formula (eqs 4 and 5) introduced previously.

The Pu atom is converged at the Hartree–Fock level to the J = 0 ground state, with 44 and 50 electrons in the g and u irreducible representations, respectively. For the hydroxy radical, the SCF calculation was performed using the average of configurations formalism,[65] with 8 electrons taken as closed shell and 1 as open shell. In the open-shell coupled cluster model, the occupations of the different irreducible representations (Ω = 1/2, −1/2, 3/2, −3/2) were restricted to be 3, 3, 1, and 0, respectively. The internuclear distance used was that obtained at the DFT level (see Geometries and Enthalpy Corrections), as was the case for H_2, H_2O, and H_2O_2.

Apart from the ground-state MP2, CCSD, and CCSD(T) calculations, we performed equation-of-motion calculations for ionization potentials (EOM-IP-CCSD) for atomic Pu and PuO_2, as well as excitation energies (EOM-EE-CCSD)[19] for PuO_2, on the basis of the coupled cluster wave functions above.

In the case of EOM-IP-CCSD for Pu, we requested the number of states as follows: five $\Omega = 1/2_g$, two $\Omega = 3/2_g$, one $\Omega = 5/2_g$, three $\Omega = 1/2_u$, two $\Omega = 3/2_u$, and one $\Omega = 5/2_u$, whereas for PuO_2 we requested two $\Omega = 1/2_g$, one $\Omega = 3/2_g$, three $\Omega = 1/2_u$, two $\Omega = 3/2_u$, and one $\Omega = 5/2_u$ states. In the case of EOM-EE-CCSD we requested the number of states as follows: six $\Omega = 0_g$, four $\Omega = 1_g$, three $\Omega = 2_g$, two $\Omega = 3_g$, one $\Omega = 4_g$, one $\Omega = 5_g$, ten $\Omega = 0_u$, nine $\Omega = 1_u$, seven $\Omega = 2_u$, five $\Omega = 3_u$, three $\Omega = 4_u$, and one $\Omega = 5_u$.

RESULTS AND DISCUSSION

Electronic Structure Analysis. *Atomic Pu.* To compute the enthalpies of formation of the plutonium molecules, an accurate description of the plutonium atom, i.e. its electronic structure, is mandatory. Thus, in Table 3 and Table S2 in the Supporting Information, the SO-CASPT2 calculations are reported and compared to available data from the literature.[45−47] The SO-CASPT2 energy levels are able to accurately reproduce the experimental assignments with errors between 91 and 397 cm^{-1} for the first five excited states below 9500 cm^{-1}. Deviations between our results and the available data appear after the sixth state; the experimental assignment predicts the sixth state at 9773 cm^{-1} with J = 0, while such a state is found at 12488 cm^{-1} in the current study, though uncertainties remain for the attribution of this electronic state. The computed seventh state with J = 6 is about 800 cm^{-1} higher in energy than the experimental value. Looking closely at the nature of the plutonium low-lying states, one can first notice the remarkable mixing among the ^7F, ^5D, and ^3P spin–

Table 3. Fine Structure Transition Energies (ΔE in cm^{-1}) of Atomic Pu Computed at the SO-CASPT2 Level with the ANO-RCC-TZVP Basis Set and Analysis of the Various J States in Terms of the Dominating LS Terms

exptl[45−47]	ΔE	J	weight of LS states
0	0	0	54% ^7F, 38% ^5D, 7% ^3P
2204	1806	1	64% ^7F, 32% ^5D
4300	4208	2	82% ^7F, 17% ^5D
6145	6353	3	88% ^7F, 10% ^5D
7775	8091	4	93% ^7F
9179	9552	5	90% ^7F
10238	11010	6	85% ^7F, 10% ^5G
9773	12499	0	44% ^7F, 21% ^5D, 8% ^3P
13528	13612	1	66% ^9H, 9% ^7F, 7% ^7G

DOI: 10.1021/acs.inorgchem.9b02096
Inorg. Chem. 2019, 58, 14507−14521

orbit free states and that the contribution of the ^{5}D state decreases as the energy increases. Finally, the most important result is the overall good reproduction of the SO splitting of the ^{7}F spin-free state, making us confident about the accuracy of the SOC for the plutonium molecules. We further note that we have the single-reference $J = 0$ ground state well described by the ^{2}DC^M-CCSD(T) method.

PuO_3 and $PuO_2(OH)_2$ Molecules. For PuO_3, at the spin−orbit level, we report the description of the ground state and the six lowest excited states in Table 4. It is noteworthy that

Table 4. Lowest Vertical Transition Energies (ΔE in cm^{-1}) of PuO_3, Computed at the SF-CASPT2 and SO-CASPT2 Levels with the ANO-RCC-TZVP Basis Set, and Analysis of the Various States

	no.	state	ΔE	character: % [orbital(number of electrons)]
SF	1	$^3B_2(1)$	0	36% [$4a_1/p^{(O)}(2)$, $1b_1/\phi_u(1)$, $1b_2/p^{(O)}(\bar{1})$, $2b_2/\sigma_u(2)$, $3b_2/\delta_u(1)$, $1a_2/\delta_u(1)$]
				21% [$4a_1/p^{(O)}(2)$, $1b_1/\phi_u(1)$, $1b_2/p^{(O)}(1)$, $2b_2/\sigma_u(2)$, $3b_2/\delta_u(\bar{1})$, $1a_2/\delta_u(1)$]
				22% [$4a_1/p^{(O)}(2)$, $1b_1/\phi_u(1)$, $1b_2/p^{(O)}(2)$, $2b_2/\sigma_u(2)$, $1a_2/\delta_u(1)$]
	2	$^3A_2(1)$	3161	43% [$4a_1/p^{(O)}(2)$, $5a_1/\phi_u(1)$, $1b_2/p^{(O)}(\bar{1})$, $2b_2/\sigma_u(2)$,$3b_2/\delta_u(1)$, $1a_2/\delta_u(1)$]
				23% [$4a_1/p^{(O)}(2)$, $5a_1/\phi_u(1)$, $1b_2/p^{(O)}(1)$, $2b_2/\sigma_u(2)$,$3b_2/\delta_u(\bar{1})$, $1a_2/\delta_u(1)$]
				17% [$4a_1/p^{(O)}(2)$, $5a_1/\phi_u(1)$, $1b_2/p^{(O)}(2)$, $2b_2/\sigma_u(2)$, $1a_2/\delta_u(1)$]
	3	$^3B_1(1)$	4663	38% [$4a_1/p^{(O)}(2)$,$5a_1/\phi_u(1)$, $1b_1/\phi_u(1)$, $1b_2/p^{(O)}(\bar{1})$, $2b_2/\sigma_u(2)$,$3b_2/\delta_u(1)$]
				12% [$4a_1/p^{(O)}(2)$, $5a_1/\phi_u(1)$, $2b_1/\pi_u(1)$, $1b_2/p^{(O)}(\bar{1})$, $2b_2/\sigma_u(2)$,$3b_2/\delta_u(1)$]
				12% [$4a_1/p^{(O)}(2)$, $5a_1/\phi_u(1)$, $1b_1/\phi_u(1)$, $2b_1/\pi_u(2)$, $1b_2/p^{(O)}(2)$]
	4	$^1A_1(1)$	7239	32% [$4a_1/p^{(O)}(2)$, $1b_2/p^{(O)}(1)$, $2b_2/\sigma_u(2)$,$3b_2/\delta_u(\bar{1})$, $1a_2/\delta_u(2)$]
				28% [$4a_1/p^{(O)}(2)$, $1b_2/p^{(O)}(2)$, $2b_2/\sigma_u(2)$, $1a_2/\delta_u(2)$]
				11% [$4a_1/p^{(O)}(1)$, $5a_1/\Phi_u(\bar{1})$, $1b_2/p^{(O)}(2)$, $2b_2/\sigma_u(2)$, $1a_2/\delta_u(2)$]
	5	$^3A_2(2)$	7287	20% [$4a_1/p^{(O)}(2)$, $1b_1/\phi_u(1)$, $1b_2/p^{(O)}(1)$, $2b_2/\sigma_u(2)$,$3b_2/\delta_u(2)$]
				18% [$4a_1/p^{(O)}(1)$,$5a_1/\Phi_u(\bar{1})$, $1b_1/\phi_u(1)$, $1b_2/p^{(O)}(2)$, $2b_2/\sigma_u(2)$,$3b_2/\delta_u(1)$]
				17% [$4a_1/p^{(O)}(2)$, $1b_1/\phi_u(1)$, $1b_2/p^{(O)}(2)$, $2b_2/\sigma_u(2)$,$3b_2/\delta_u(1)$]
	6	$^3B_1(2)$	8038	31% [$4a_1/p^{(O)}(1)$,$5a_1/\Phi_u(\bar{1})$, $1b_2/p^{(O)}(2)$, $2b_2/\sigma_u(2)$,$3b_2/\delta_u(1)$, $1a_2/\delta_u(1)$]
				11% [$4a_1/p^{(O)}(2)$,$5a_1/\phi_u(1)$, $2b_1/\pi_u(1)$, $1b_2/p^{(O)}(\bar{1})$, $2b_2/\sigma_u(2)$,$3b_2/\delta_u(1)$]
				10% [$4a_1/p^{(O)}(2)$, $1b_2/p^{(O)}(2)$, $2b_2/\sigma_u(2)$,$3b_2/\delta_u(1)$, $1a_2/\delta_u(1)$]
				10% [$4a_1/p^{(O)}(2)$, $1b_1/\phi_u(1)$, $2b_1/\pi_u(1)$, $1b_2/p^{(O)}(\bar{1})$, $2b_2/\sigma_u(2)$, $1a_2/\delta_u(1)$]
SO		X	0	47% $(1)^3B_2$ + 24% $(1)^3A_2$ + 14% $(1)^3B_1$
		a	1235	59% $(1)^3B_2$ + 25% $(1)^3A_2$
		b	1783	73% $(1)^3B_2$
		c	3777	51% $(1)^3A_2$
		d	5660	24% $(1)^3B_1$ + 18% $(1)^1A_1$ + 17% $(2)^3A_2$ + 10% $(2)^3B_1$

the $1a_g$, $2a_g/\delta_u$, and $3a_g$ orbitals are doubly occupied in all of the calculated spin-free states. The PuO_3 orbitals are composed of a mixture of orbitals belonging to the plutonyl subunit and the distant oxygen. Thus, for the sake of clarity, we label these orbitals with those normally associated with the PuO_2^{2+} ion (with linear energy D_{2h} notations), and those of the distant oxygen atom are denoted by $p^{(O)}_{x,y,z}$. The SO ground state is composed of 47% $^3B_2$, 24% $^3A_2$, and 14% $^3B_1$ spin-free states. The composition is similar to that previously reported by Kovács[66] (52% $^3B_2$ and 24% $^3A_2$). More striking is the difference between our computed vertical excitation energies with that of Kovács' SO-CASPT2 spectrum.[66]

We predict the first excited state to be at 1235 cm^{-1}, in contrast to the 471 cm^{-1} previously found,[66] and the overall spectrum determined from our calculations is much denser and lower by about 4000 cm^{-1} than in ref 66. Such discrepancy may find its origin in the description of the spin-free states. Although we agree with Kovács that the spin-free ground state has $^3B_2$ symmetry, we find a different orbital character. In our calculations, the $^3B_2$ exhibits a strong multideterminantal character with 57% corresponding to the configuration in which the $4a_1/p^{(O)}_z$ and $2b_2/\sigma_u$ orbitals are doubly occupied (see Table 4 and Figure 1) and the singly occupied orbitals $5b_1/\Phi_u$, $1b_2/p^{(O)}_z$, $3b_2/\delta_u$, and $1a_2/\delta_u$ and 22% from the electronic configuration in which of the $4a_1/p^{(O)}_z$, $1b_2/p^{(O)}_z$ and $2b_2/\sigma_u$ orbitals are doubly occupied and the $5b_1/\Phi$ and $1a_2/\delta_u$ singly occupied. Kovács, however, finds the ground state to be mainly composed of plutonyl orbitals (79%).

Such a difference can be explained by the fact that the considered active spaces are different, CAS(10,16) in his case and CAS(14,13) in our work. In a close look at the entanglement diagram of PuO_3 derived from DMRG calculations[10] (Figure 6a, Full-Valence CAS of ref 10) there is a strong correlation within the nonbonding plutonyl-like orbitals (δ_u, ϕ_u) and also between the $b_2/p^{(O)}$ and the $5f\delta_u$ orbitals, in agreement with our analysis of the $^3B_2$ ground-state wave function.

Concerning $PuO_2(OH)_2$ (Figure 2), the low-energy part of the vertical spectrum including SOC reported in Table 5 shows two close-lying states separated by about 323 cm^{-1}, followed by a state at 2222 cm^{-1}. The analysis of the two lowest states indicates that they correspond to a 50−50 combination of $(1)^3A$ and $(1)^3B$ spin-free states, with a small contribution of the $(2)^3B$ (6% in each case). The next three states also have strong mixings induced by SOC between triplet states but also singlet excited states of $(1)^1A$ and $(1)^1B$ symmetries, placed at the spin-free level at about 5764 and 7444 cm^{-1}, respectively.

PuO_2 and PuO_2^+ Molecules. At the ^{2}DC^M level, the PuO_2 ground state is found to be well-described by a closed-shell ($\Omega = 0^+_g$) determinant, corresponding to occupied $5f_{-3/2;+3/2}$, $5f_{-5/2;+5/2}$ spinors. We note that the T_1 diagnostic is 0.03, a value very similar to that found for single-reference uranium molecules.[16] This allowed us to employ accurate two-component single-reference approaches such as CCSD(T) to determine the optimal Pu−O bond length after CBS extrapolation to be 1.808 Å, with a corresponding harmonic vibrational symmetric stretching frequency of 791 cm^{-1} (the antisymmetric stretching and bending frequencies being 840 and 170 cm^{-1}, respectively). We note that these results are in excellent agreement with the scalar relativistic CCSD(T) geometry (1.814 Å) and harmonic frequencies (147, 777, 825 cm^{-1}) reported by Feng and Peterson,[67] who agree with us that PuO_2 ground state has a 0^+_g character with a distance longer than that (1.744 Å) predicted by La Macchia et al.[50,68] at the SO-CASPT2 level, though for the chemically different ground state $^5\Phi_u$.

Furthermore, our ^{2}DC^M-EOM-EE-CCSD calculations (see Table 6) confirm that, at the CBS-^{2}DC^M-CCSD(T) equilibrium structure, the $\Omega = 0^+_g$ state is indeed the ground state: it is sufficiently well separated from the lowest-lying states of

DOI: 10.1021/acs.inorgchem.9b02096
Inorg. Chem. 2019, 58, 14507−14521

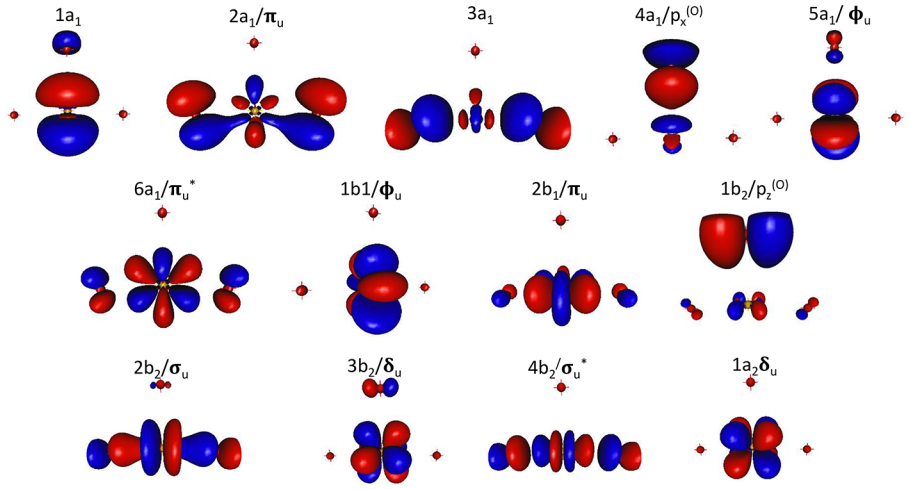

Figure 1. Active CASSCF orbitals of PuO_3 at the CASSCF level. Isosurface: 0.05 au. Distances: Pu−O(PuO_2^{2+}subunit) = 1.767 Å; Pu−O_{axial} = 1.934 Å; angle(O−Pu−O_{axial}) = 93.86°.

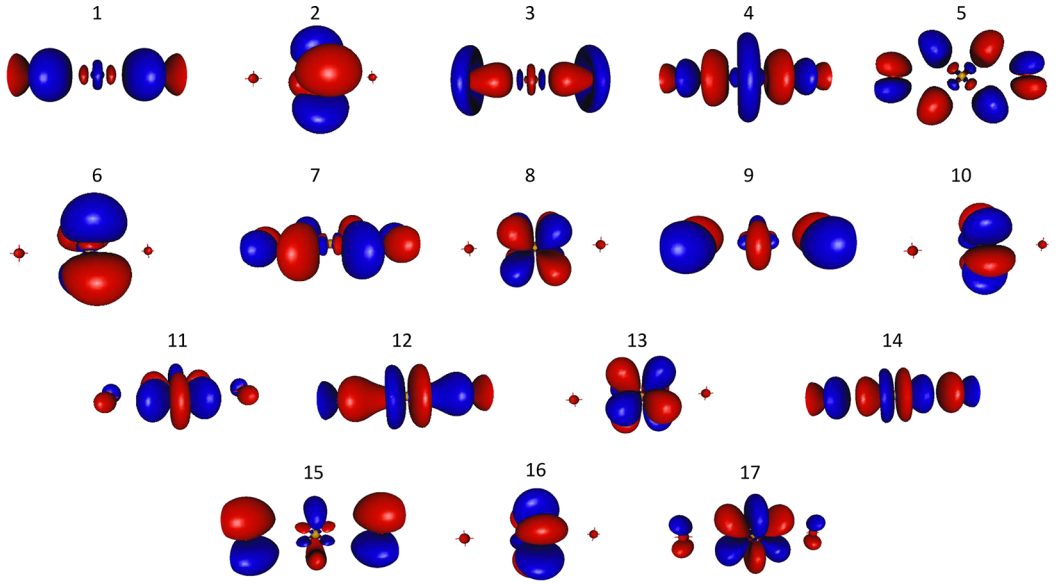

Figure 2. Molecular orbitals of $PuO_2(OH)_2$ at CASSCF level. Isosurface: 0.05 au. Distances: Pu−OH = 2.103 Å, Pu−O = 1.742 Å; Angles: O−Pu−OH = 92.15°; HO−Pu−OH = 105.68°; O−Pu−O = 174.29°.

both g ($\Omega = 1_g$, by over 2000 cm^{-1}) and u ($\Omega = 1_u$, by over 5000 cm^{-1}), and considering a shorter bond length, namely 1.744 Å, as was proposed by La Macchia et al.[50] for the ground state from SO-CASPT2 calculations, does not alter this picture. Thus, our results differ qualitatively and quantitatively from ref 50, which found the PuO_2 ground state to be of $\Omega = 1_u$ symmetry, corresponding to the occupation of the two δ_u, one ϕ_u, and the 7s orbitals (see Figure 3).

From Table 6, we observe significant variations for the u states (of nearly 3000 cm^{-1}) when the internuclear distance is shortened from 1.808 to 1.744 Å, while the g states remain more or less at the same energies. With this, at this longer distance, the $\Omega = 2_g$ state becomes lower than the $\Omega = 1_u$ state.

The SO-CASPT2 transition energies computed at the $^2DC^M$ optimal bond length are reported in Tables 6 and 7 and Table S5 in the Supporting Information. The spin−orbit 0_g^+ ground state is composed by the spin-free ground state $(1)^5\Sigma_g^+$ up to 48% and by $(1)^3\Sigma_g^-$ up to 22%, which lies 10308 cm^{-1} above it. Note that the current vertical transition energies computed at the SO-CASPT2 level are in very good agreement with the $^2DC^M$ energies for the g states, but the u manifold come out about 4000 cm^{-1} lower in energy at the SO-CASPT2 level than at the $^2DC^M$-EOM-CCSD level. The fact that the $0_g^+ - 1_u$ energy difference computed at the SO-CASPT2 level of theory (5851 cm^{-1}) agrees best with the spin−orbit corrected CCSD(T) value by Feng and Peterson (5421 cm^{-1}) than with the $^2DC^M$-EOM-CCSD value suggests that triple corrections have a large contribution to such g to u transitions involving a change in Pu orbital occupations. Thus, all levels of theory predict the ground state to have 0_g^+ symmetry at both shorter and longer Pu−O distances, disagreeing with the proposed 1_u nature of the ground state by La Macchia et al.[50] However, we note that the electronic state spacing within either the g or u symmetries agrees in both SO-CASPT2 calculations. This finding points out to the importance of the choice of the active space to accurately predict the relative energies of g states involving mostly nonbonding 5f Pu atomic-

DOI: 10.1021/acs.inorgchem.9b02096
Inorg. Chem. 2019, 58, 14507−14521

Table 5. Lowest Vertical Transition Energies (ΔE in cm^{-1}) of $PuO_2(OH)_2$, Computed at the SF-CASPT2 and SO-CASPT2 Levels with ANO-RCC-TZVP Basis Sets, and Analysis of the Various States

	state	ΔE	character: % [orbital(number of electrons)]
SF	$(1)^3B$	0	49% [2a/ϕ_u(1), 1b/δ_u(1)]
			48% [1a/δ_u(1), 2b/ϕ_u(1)]
	$(1)^3A$	889	41% [1a/δ_u(1), 2a/ϕ_u(1)]
			59% [1b/δ_u(1), 2b/ϕ_u(1)]
	$(2)^3B$	2136	75% [1a/δ_u(1), 1b/δ_u(1)]
			20% [2a/ϕ_u(1), 2b/ϕ_u(1)]
	$(2)^3A$	4698	59% [1a/δ_u(1), 2a/ϕ_u(1)]
			41% [1b/δ_u(1), 2b/ϕ_u(1)]
	$(3)^3B$	5351	52% 2a/ϕ_u(1), 1b/δ_u(1)
			46% [1a/δ_u(1), 2b/ϕ_u(1)]
	$(1)^1A$	5764	58% [1b/δ_u(1), 2b/$\Phi_u(\bar{1})$]
			30% [1a/δ_u(1), 2a/$\Phi_u(\bar{1})$]
			5% [2a/ϕ_u(2)]
	$(1)^1B$	7444	50% [1a/δ_u(1), 1b/$\delta_u(\bar{1})$]
			28% [2a/ϕ_u(1), 2b/$\Phi_u(\bar{1})$]
			16% [1a/δ_u(1), 2b/$\Phi_u(\bar{1})$]
	$(2)^1A$	9626	39% [1a/δ_u(1), 2a/$\Phi_u(\bar{1})$]
			29% [2a/ϕ_u(2)]
			13% [1b/δ_u(1), 2b/$\Phi_u(\bar{1})$]
			10% [1a/δ_u(2)]
			7%[2a/ϕ_u(2)]
SO	X	0	46% $(1)^3A$, 41% $(1)^3B$, 6% $(2)^3B$
	a	323	45.% $(1)^3B$, 45% $(1)^3A$, 6% $(2)^3B$
	b	2222	35% $(2)^3B$, 25% $(1)^3B$, 14% $(1)^1A$, 13% $(2)^3A$, 10% $(3)^3B$
	c	3757	40% $(2)^3A$, 25% $(2)^3B$, 19% $(1)^1B$, 7% $(1)^3B$, 6% $(1)^3A$
	d	4158	36% $(3)^3B$, 34% $(2)^3B$, 14% $(2)^1A$, 11% $(1)^3B$

Table 6. Comparison of CBS Extrapolated $^2DC^M$-EOM-CCSD and SO-CASPT2 PuO_2 Vertical Transition Energies (ΔE in cm^{-1}) Computed at the 1.744 and 1.808 Å Pu−O Distances

	d(Pu−O) = 1.744 Å			d(Pu−O) = 1.808 Å	
Ω		SO-CASPT2			
	$^2DC^M$-EOM-CCSD ΔE	ΔE	ΔE[50]	$^2DC^M$-EOM-CCSD ΔE	SO-CASPT2 ΔE
0_g^+	0	0	1794	0	0
1_g	2554	1438	2315	2457	2462
2_g	6366	4235	4131	5663	5904
0_g	7138			7134	
3_g	9480			9073	
1_g	10098			9502	
0_g	10195			10415	
1_u	7011	1778	0	9822	5851
2_u	7225	1805	535	10057	6265
2_u	7653			10854	
3_u	7955			11214	
4_u	13531			16236	

centered orbitals, versus the u states involving the more diffuse Pu 7s orbital.

In addition to calculations including SOC, it is informative to discuss the nature of the PuO_2 ground state without SOC. Our CASPT2 and UCCSD(T) calculations place the $^5\Sigma_g^+$ state ($(\delta_u)^2(\phi_u)^2$ occupations) lower in energy than the $^5\Phi_u$ state ($(\delta_u)^2(\phi_u)^1(7s)^1$) by 7994 cm^{-1} at a Pu−O distance of 1.808 Å, as found in the previous studies.[50,69] With the ANO-RCC AVTZ basis set, the equilibrium Pu−O distances are 1.818 and 1.808 Å at the UCCSD(T) and CASPT2 levels, respectively, distances that are close to the $^2DC^M$-CCSD(T) result. These values are also in line with the SF-CASPT2 (CAS(12,14)) of La Macchia (d(Pu−O)) = 1.792 Å) but significantly shorter (by about 0.04/0.05 Å) than the estimations of Archibong and Ray.[69] The large discrepancies observed with respect to the latter are probably related to the choice of a large-core RECP (78 electrons), which yields bond distances in actinide molecules that are too long,[70] while the small-core ECP gives exactly the same distances as the all-electron Douglas−Kroll relativistic approach.

The ground state $(1)^5\Sigma_g^+$ is dominated (84%) by the configuration in which the two $5\delta_u$ and two ϕ_u orbitals carry one electron each. It corresponds to the description of the ground state of Boguslawski et al.[10] and by Feng and Peterson,[67] and also to the $(1)^5\Sigma_g^+$ state reported by La Macchia et al.[50] The former study places the first excited state at 1800 cm^{-1} corresponding to the $^5\Phi_u$ state, while in our SF-CASPT2 calculation it appears at a higher energy (5421 cm^{-1}). We note that in our SF-CASPT2 calculation the spectrum is less dense than in La Macchia's results.[50] Such differences can be explained by the choice of different active spaces, by the fact that we computed a larger number of spin-free states, and most likely by the change in the interatomic Pu−O distance. SOC is not expected to change the energy of the $\Omega = 0_g^-$ state, while it lifts the degeneracy of the $^5\Phi_u$ state, giving rise to three (1_u, 2_u, and 3_u) fine structure states, split by 2133 cm^{-1} (See Table 4 of ref 50). Given the small energy gap of 1800 cm^{-1} in La Macchia's[50] study between the $^5\Sigma_g^+$ and $^5\Phi_u$ states, the 1_u state becomes the ground state, while in our work, it remains a state of gerade symmetry (0_g^+), unambiguously confirmed by the $^2DC^M$ calculations.

Apart from determining the excitation energies for PuO_2, the EOM-CCSD method is also useful to investigate the ionization potentials of PuO_2, for which there are experimental data. Being a relative measure, this can help to validate $^2DC^M$-EOM-CCSD as a reliable approach with which to benchmark SO-CASPT2. The computed vertical and adiabatic ionization energies (IPs; see Table 8) can be grouped into three regions with respect to their energies: two below 8 eV, one between 8 and 10 eV, and the last at energies higher than 10 eV. The lowest EOM-IP-CCSD state has $\Omega = 3/2_u$ symmetry, as found by Feng and Peterson,[67] with an adiabatic IP of 7.07 eV, in very good agreement with the SO-CCSD(T) value (6.93 eV),[67] and within the error bar of the adiabatic value (7.03 ± 0.12) eV, measured by Santos et al.[22] However, the values reported by Rauh et al.[20] and Capone et al.,[21] lying at 9.4 ± 0.5 and (10.1 ± 0.1) eV, respectively. would match the value we computed for the first $\Omega = 1/2_u$, leading us to suggest that these experiments may have measured PuO_2^+ in different electronically excited states.

The calculated electronic states of PuO_2^+ correspond to ionizations from the nonbonding δ_u ($\Omega = 3/2_u$) and ϕ_u ($\Omega = 5/2_u$) and from the bonding σ_u ($\Omega = 1/2_u$) and π_u ($\Omega = 3/2_u$). In the first two cases, as we do not alter the number of bonding spinors, the removal of an electron increases the Pu−O bond energy, as can be seen by the decreased equilibrium bond length and higher harmonic vibrational stretching frequencies in comparison to the CCSD values (r_e(Pu−O) = 1.792 Å; ω_e = 833 cm^{-1}) for PuO_2 (by about 0.095 Å and 177 cm^{-1} for $\Omega = 3/2_u$ and 0.104 Å and 202 cm^{-1} for $\Omega = 5/2_u$).

DOI: 10.1021/acs.inorgchem.9b02096
Inorg. Chem. 2019, 58, 14507−14521

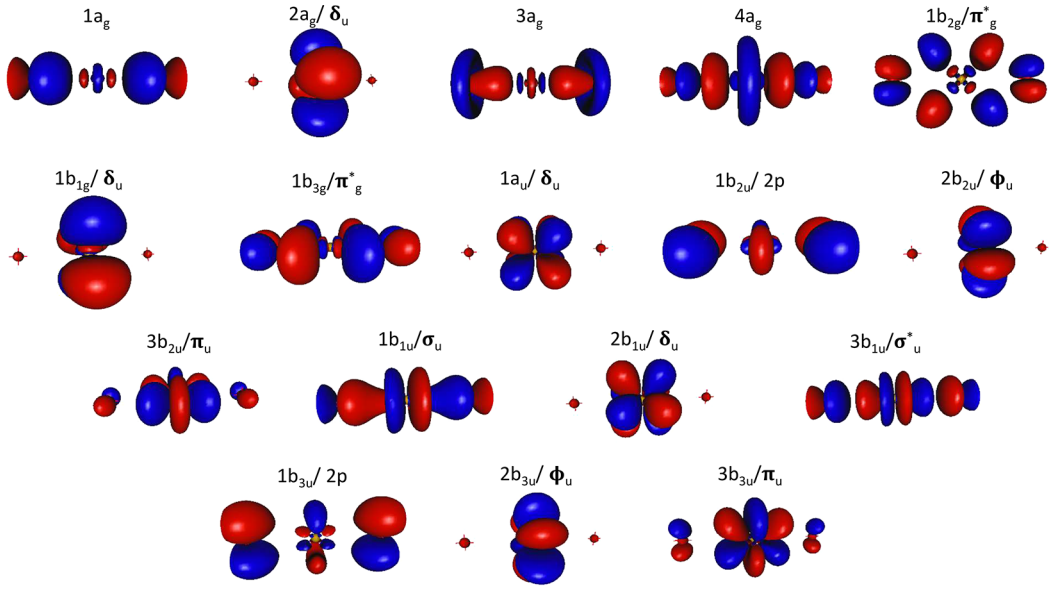

Figure 3. Molecular orbitals of PuO_2 at the CASSCF level. r(Pu−O) = 1.808 Å. Isosurface: 0.05 au.

Table 7. Lowest Vertical Transition Energies (ΔE in cm^{-1}) of PuO_2, Domputed at the SF-CASPT2 and SO-CASPT2 Levels (d(Pu−O) = 1.808 Å) with ANO-RCC-TZVP Basis Sets, and Analysis of the Various States

	state	ΔE	character: % [orbital(number of electrons)]
SF	$(1)^5\Sigma_g^+$	0	84% [1a$_u$/δ$_u$(1), 2b$_{2u}$/ϕ$_u$(1), 2b$_{1u}$/δ$_u$(1), 2b$_{3u}$/ϕ$_u$(1)]
	$(1)^5\Sigma_g^-$	4798	45% [1a$_u$/δ$_u$(1), 3b$_{2u}$/π$_u$(1), 2b$_{1u}$/δ$_u$(1), 2b$_{3u}$/ϕ$_u$(1)]
			45% [1a$_u$/δ$_u$(1), 2b$_{2u}$/ϕ$_u$(1), 2b$_{1u}$/δ$_u$(1), 3b$_{3u}$/π$_u$(1)]
	$(1)^5\Phi_u$	5421	85% [3a$_g$(1), 1a$_u$/δ$_u$(1), 2b$_{1u}$/δ$_u$(1), 2b$_{3u}$/ϕ$_u$(1)]
	$(1)^5\Delta_u$	7452	79% [3a$_g$(1), 2b$_{2u}$/ϕ$_u$(1), 2b$_{1u}$/δ$_u$(1), 2b$_{3u}$/ϕ$_u$(1)]
	$(1)^3\Sigma_g^-$	10308	24% [1a$_u$/δ$_u$(1), 2b$_{2u}$/ϕ$_u$(2), 2b$_{1u}$/δ$_u$(1)], 24% [1a$_u$/δ$_u$(1), 2b$_{1u}$/δ$_u$(1), 2b$_{3u}$/ϕ$_u$(2)], 19% [2b$_{2u}$/ϕ$_u$(1), 2b$_{1u}$/δ$_u$(2), 2b$_{3u}$/ϕ$_u$(1)], 16% [1a$_u$/δ$_u$(1), 2b$_{2u}$/ϕ$_u$(1), 2b$_{3u}$/ϕ$_u$(1)]
SO	0_g^+	0	48% $(1)^5\Sigma_g^+$, 22% $(1)^3\Sigma_g^-$
	1_g	2462	67% $(1)^5\Sigma_g^+$, 15% $(1)^3\Sigma_g^-$
	1_u	5851	27% $(1)^5\Phi_u$, 27% 21% $(2)^5\Phi_u$, 13% $(1)^5\Delta_u$, 13% $(2)^5\Delta_u$
	2_g	5904	85% $(1)^5\Sigma_g^+$
	2_u	6265	21% $(1)^5\Phi_u$, 21% $(2)^5\Phi_u$, 24% $(1)^5\Delta_u$
	3_u	7195	39% $(1)^5\Phi_u$, 25% $(2)^5\Phi_u$

Table 8. CBS Extrapolated Vertical and Adiabatic Ionization Potentials (IPs in eV) of PuO_2 Computed at the $^2DC^M$-EOM-IP-CCSD Level[a]

$^2DC^M$-EOM-IP-CCSD				
state	IP$_{vert}$	IP$_{adiab}$	r_e	ω_e
3/2$_u$	7.67	7.07	1.697	1010
5/2$_u$	7.93	7.20	1.688	1035
1/2$_u$	9.81	9.77	1.771	811
3/2$_u$	10.80	10.79	1.831	940
Theoretical				
		IP$_{adiab}$	ref	
X2C-DC-CCSD(T)		5.93	68	
SO-CCSD(T)		6.93	67	
Experimental				
IP$_{adiab}$		ref		
9.4 ± 0.5		20		
10.1 ± 0.1		21		
7.03 ± 0.12		22		
6.6[b]		71, 72		

[a]The interatomic distance (r_e(Pu−O) = 1.808 Å, from $^2DC^M$-CCSD(T) calculations) was used for the vertical IPs, while the adiabatic IPs correspond to the reported equilibrium r_e distances of PuO_2^+ and harmonic symmetric stretching ω_e frequencies. Experimental and other theoretical values correspond to adiabatic IPs. [b]Rejected value according to the comment by Gibson et al.[72] on Capone et al.'s measurements.[71]

The other two states, on the other hand, can be seen as excited states where the electrons from the bonding σ_u and π_u spinors are excited to the nonbonding δ_u, and as such the net bonding interaction is reduced in the molecule, whereas for the second $\Omega = 3/2_u$ there is an increase in bond length and in frequency in comparison to the PuO_2 CCSD(T) values (by 0.039 Å and 107 cm^{-1}). Finally, for the $\Omega = 1/2_u$, we observe a slight decrease in bond length (of 0.021 Å) together with a slight decrease in vibrational frequency (of 21 cm^{-1}) in comparison to the PuO_2 CCSD(T) values.

Taken together, our $^2DC^M$-EOM-CCSD calculations show it can be used to assess the SO-CASPT2 method for energy differences.

Thermodynamic Data. All of the results so far have demonstrated the accuracy and reliability of the $^2DC^M$-CCSD approach and the relative accuracy of SO-CASPT2. Now, we can proceed with the determination of the thermodynamic data. Recently, a thorough assessment of the thermodynamic properties of gaseous plutonium oxides has been done by Konings et al.[2] The derived functions (entropy and heat capacity) have been calculated on the basis of the most reliable data available in the literature. Nevertheless, the authors pointed out a number of missing data, especially regarding the contributions of electronically excited states.

In the following, from results discussed before and the related molecular parameters and electronic states (see Tables S7−S9 in the Supporting Information), the heat capacity and

DOI: 10.1021/acs.inorgchem.9b02096
Inorg. Chem. 2019, 58, 14507−14521

the standard entropy of $PuO_2(g)$, $PuO_3(g)$, and $PuO_2(OH)_2(g)$ are thus derived and compared to those selected by Konings et al.[2] or calculated by Ebbinghaus.[73] Regarding the standard heat of formation, an analysis of transpiration measurements made by Krikorian et al.[5] was performed to extract values of $PuO_3(g)$ and $PuO_2(OH)_2(g)$, whereas for $PuO_2(g)$, our results are analyzed in the light of Konings' assessment.[2]

From the discussions on the previous sections of the electronic structures of the different Pu species, one will not be surprised to see that the single-reference methods, DFT and CC, fail at describing standard heats of formation of $PuO_2(OH)_2$ and PuO_3, while it should be in principle applicable for PuO_2. For the latter, data obtained by coupled-cluster calculations are therefore used to establish its thermodynamic properties, whereas regarding the other species, multireference results are used.

$PuO_2(g)$. Let us first discuss the thermodynamic functions of PuO_2. Regarding the standard entropy at room temperature, an analysis of the sources of discrepancies between our calculation and up to date data from the literature reveals that vibrational and electronic partition functions are in disagreement (see Table S10 in the Supporting Information).

In the thermodynamic review of Konings et al.,[2] although information on the PuO_2 electronic states could have been taken from La Macchia et al.,[50] the contributions to the entropy of the PuO_2 electronic states were estimated by considering the crystal-field split $5f^2$ energy levels of $PuF_4(cr)$, which are densely spaced, thus leading to a significant overestimation of the electronic contributions to entropy. Regarding the vibrational contributions, Konings et al.[2] used the harmonic frequencies computed at the scalar relativistic CCSD(T) level by Archibong and Ray.[69] Our $^2DC^M$-CCSD(T) harmonic stretching frequencies (791 and 840 cm^{-1}) are very close to their CCSD(T) values (792 and 828 cm^{-1}) and to the DKH3-CCSD(T) values of Feng and Peterson[67] (777 and 825 cm^{-1}); the bending frequency comes out slightly higher in our calculation (170 cm^{-1}) than in previous reports (106 cm^{-1} [69] and 147 cm^{-1} [67]), probably due to the inclusion of spin−orbit coupling. As a result our thermodynamics function differs from that proposed by Konings et al.[2] Unfortunately, except for the asymmetric stretching mode by infrared absorption spectroscopy[74] of PuO_2 in Ar and Kr matrices (794.25 and 786.80 cm^{-1}), the other vibrational frequencies are unknown, making it impossible to assess the accuracy of the currently reported quantum chemical frequencies. Our calculated standard entropy at room temperature is thus equal to

$$S^{\ominus}_{298K} = 262.9\ \mathrm{J\ K^{-1}\ mol^{-1}} \tag{6}$$

which is lower by about 16 J K^{-1} mol^{-1} than the value in the assessment of Konings et al. (278.7 J K^{-1} mol^{-1}).[2] An analogous discussion can be made as to the effect of the PuO_2 electronic states on the heat capacity (see Figure S1 in the Supporting Information). At room temperature, Konings et al.[2] reported a $C_p^{\ominus}(T)$ value higher than ours by tens of J K^{-1} mol^{-1}, due to their overestimated excited-state contributions. The heat capacity function of the present work (in J K^{-1} mol^{-1}) is expressed as

$$C_p^{\ominus}(T) = 42.7970 + (3.5713 \times 10^{-2})(T/K) - (1.2077 \times 10^{-5})(T/K)^2 - (2.0271 \times 10^{5})(T/K)^{-2} \tag{7}$$

in the 298.15−1200 K temperature range and becomes

$$C_p^{\ominus}(T) = 54.1604 + (1.2436 \times 10^{-2})(T/K) - (1.7456 \times 10^{-6})(T/K)^2 + (2.2335 \times 10^{6})(T/K)^{-2} \tag{8}$$

in the 1200−3000 K range.

Coming now to the standard enthalpy of formation of PuO_2, we first note that the value we report in Table 9 from B3LYP calculations including the spin−orbit + ΔE_{SO} correction is about 25% off (100 kJ mol^{-1}) the experimental value. A change in the density functional will not ensure a better agreement with experiment, as observed previously for actinide systems[75] or for transition-metal molecules.[76] Thus, we will rely on wave function based approaches to propose revised values of $\Delta_f H^{\ominus}$ (298.15 K) and will take the CBS-corrected $^2DC^M$-CCSD(T) result to be the best estimate for the standard heat of formation of $PuO_2(g)$, yielding

$$\Delta_f H^{\ominus}(298.15\ \mathrm{K}) = -449.5 \pm 8.8\ \mathrm{kJ\ mol^{-1}} \tag{9}$$

In addition, by combining the $^2DC^M$-CCSD(T) standard enthalpy of formation of PuO_2 with the $^2DC^M$-EOM-IP-CCSD value of its adiabatic ionization potential IE(PuO_2), we can predict the standard enthalpy of formation of PuO_2^+ through the relation

$$\Delta_f H^{\ominus}[PuO_2^+] = \Delta_f H^{\ominus}[PuO_2] + \mathrm{IE}[PuO_2] + H^{\ominus}(298.15\ \mathrm{K})[PuO_2^+] - H^{\ominus}(298.15\ \mathrm{K})[PuO_2][PuO_2^+] = 234.9 \pm 8.3\ \mathrm{kJ\ mol^{-1}} \tag{10}$$

The SO-UCCSD(T) value (−411.2 ± 6.6 kJ mol^{-1}) for $\Delta_f H^{\ominus}[PuO_2]$ roughly agrees with both the latter and experiment, but it is lower than the CBS-$^2DC^M$-CCSD(T) value (−449.5 ± 8.8 kJ mol^{-1}) by about 38 kJ mol^{-1}. The importance of the perturbative triple contributions in the electronic correlation treatment is highlighted by comparing these results to the CCSD results (see Table 9), as the one-step and two-step models show differences of 40 and 58 kJ mol^{-1}, respectively. The difference between the SO-UCCSD(T) and $^2DC^M$-CCSD(T) methods could be explained by a possible underestimation of the SOC contribution in the two-step approach, yielding a $\Delta_f H^{\ominus}$(298.15 K) value higher by about 30 kJ mol^{-1}. The SO-CASPT2 value ($\Delta_f H^{\ominus}$(298.15 K) = −413.7 ± 18.3 kJ mol^{-1}) reported in Table 9 deviates by about 36 kJ mol^{-1} from both $^2DC^M$-CCSD(T) and experiments and by about 2 kJ mol^{-1} from the SO-UCCSD(T) value, therefore showing a fair agreement with the most accurate methods. This is mirrored in the closeness of the PuO_2 atomization energies (reverse of reaction R2), reported in Table S11 in the Supporting Information. With this we concluded that perturbative approaches ($^2DC^M$-CCSD(T) and SO-CASPT2) yield reasonable results and thus could be used for other systems, though with larger uncertainties for SO-CASPT2 than for $^2DC^M$-CCSD(T).

DOI: 10.1021/acs.inorgchem.9b02096
Inorg. Chem. 2019, 58, 14507−14521

Table 9. Standard Enthalpies of Formation ($\Delta_f H^\ominus$(298.15 K) in kJ mol^{-1}) of PuO_2, $PuO_2(OH)_2$, and PuO_3 in the Gas Phase Calculated at Various Levels of Theory and Extrapolated to the Complete Basis Set (CBS) limit, Obtained from the Average over the Six Reactions Given in Table 1, except for $^2DC^M$-CCSD(T), for Which the Average Only Includes the Four Reactions R3−R6[a]

method	PuO_2	PuO_3	$PuO_2(OH)_2$
ΔE_{SO}[b]	34.4	59.0	46.9
SO-B3LYP[c]	−318.4 ± 20.6	−405.7 ± 22.5	−801.9 ± 30.3
SO-UCCSD	−353.3 ± 16.2	NC	NC
SO-UCCSD(T)	−411.2 ± 6.6	NC	NC
$^2DC^M$-CCSD[d]	−409.3 ± 14.9	NC	NC
$^2DC^M$-CCSD(T)[d]	**−449.5 ± 8.8**	NC	NC
SO-CASPT2	−413.7 ± 18.5	**−553.2 ± 27.5**	**−1012.6 ± 38.1**
experiment	−410 ± 20;[83] −428.7 ± 7[77]	−562.8 ± 5[5]	−1018.2 ± 3.3[5]
	−440 ± 7;[77] −412 ± 20[84]	−567.6 ± 15[2]	
	−428.7 ± 20[2]		

[a] ΔE_{SO} represents the spin-orbit contribution to the enthalpy, which is included in all SO-method results. The uncertainties $\Delta\Delta_f H^\ominus$ corresponding to 95% confidence intervals are computed with the formulas[82] given in the Supporting Information. [b] ΔE_{SO} is the estimate of the SO contribution. [c] The energies of reactions were estimated with a RECP and the associated basis set of triple-ζ quality for the plutonium. Thus, no CBS was performed. [d] Uncertainties over the four reactions R_3−R_6.

Going back to the available literature data, the $\Delta_f H^\ominus$(298.15 K) computed with the $^2DC^M$-CCSD(T) approach is in almost perfect agreement with the available results that correspond to the highest values for the formation enthalpy in Table 9.[2,77] The SO-CASPT2(4,4) value exhibits a rather good agreement with the selected one in the Konings assessment[2] (the value has been obtained by a second law method applied to experiments published in ref 77). This is motivated by the statement that the values obtained by third or second law analysis are not fully in agreement,[2,77] revealing a lack of consistency of experimental data.

Therefore, in future studies, experimental data can be scrutinized in regard to the present thermodynamic functions of PuO_2. The crosscheck between data from molecular parameters and standard heat of formation from quantum chemistry calculations as well as values from experiments calls for further assessments.

PuO_3(g). As highlighted in the case of the PuO_2(g) molecule, the uncertainties related to the entropy and heat capacity functions stem from the electronic partition functions. Ebbinghaus[73] and Konings et al.[2] both used the electronic spectra of PuO_2^{2+} to estimate that of PuO_3.[8,78] The latter approximation is found here to be strong, even if both our calculations and the studies by Konings et al.[2] and Ebbinghaus[73] consider that the ground state is dominated by triplet spin-free states. Indeed, while Konings et al. only considered four states from the calculations of Infante et al.,[8] we find seven states below 8000 cm^{-1}.

Regarding the vibrational contributions, the estimate used by these authors and based on an analogy with UO_3(g) seems to be acceptable because of a fortuitous good agreement, as highlighted by our calculations. The improvements of the electronic partition function lead to a weak decrease (see Table S10 in the Supporting Information) of the standard entropy at room temperature, and is thus equal to

$$S^\ominus_{298K} = 310.98 \text{ J K}^{-1} \text{ mol}^{-1} \quad (11)$$

and the heat capacity function of PuO_3(g) (in J K^{-1} mol^{-1}) is

$$C_p^\ominus(T) = 43.0757 + (1.0927 \times 10^{-1}(T/K) - 7.1581 \times 10^{-5}(T/K)^2 - 7.1469 \times 10^4(T/K)^{-2} \quad (12)$$

for the 298.15−550 K temperature range and

$$C_p^\ominus(T) = 98.1101 - (1.1768 \times 10^{-2})(T/K) + (4.5533 \times 10^{-6})(T/K)^2 - (3.5486 \times 10^6)(T/K)^{-2} \quad (13)$$

in the 550−2400 K range.

The only available experimental data of PuO_3(g) for which its standard heat of formation has been obtained comes from the transpiration method of plutonium oxide under an oxygen atmosphere.[5] The involved species is postulated from an analogy with uranium, and under the experimental conditions (under purely oxygen flow), PuO_3 is expected to be the major volatile species (under a purely oxygen flow). In this type of apparatus, the partial pressure of target species is obtained by an indirect method (measure of transported masses), which may cause a bias in the present case due to a potential contamination of the results by the ash transport (pointed out by the authors of ref 79). Nevertheless, one set of measures has been obtained with another apparatus configuration in which a silica wool glass filter has been added between the crucible and the collector tube (in a region where the temperature remains high).

Strangely, these obtained data are excluded because the following postulate has been made by authors: the lowest plutonium volatility is due to an interaction between its vapor and silica wool. Therefore, the standard heat of formation retained by the authors (−562.8 kJ mol^{-1})[5] has been obtained with the set without a silica wool filter. However, one can make the assumption that the filter traps the ash. As the filter is located in a hot zone, in the vicinity of the crucible, one can postulate that only vapor species pass through the filter without modifying the equilibrium. Thus, the data set obtained with a filter may be more accurate than that without a silica wool filter.

Taking advantage of our improved entropy and heat capacity for the PuO_3 molecule, we can reanalyze the experimental data using our ab initio data. The treatments by the third law method with the proper Gibbs energy functions of PuO_2(c)[2] and one from our adopted data for PuO_3(g) lead to the following $\Delta_f H^\ominus$ values: −572 ± 12.1 kJ mol^{-1} from the data set without a silica wool filter and 534 ± 18.5 kJ mol^{-1} with it (the uncertainties are given within a level of confidence of 95%). The former slightly differs from the original value (−562.8 kJ mol^{-1}),[5] due to our improvement of the standard entropy for PuO_3(g). We propose that the standard heat of formation computed within the SO-CASPT2 approach can be considered as the best estimated data:

$$\Delta_f H^\ominus(298.15 \text{ K}) = -553.2 \pm 27.5 \text{ kJ mol}^{-1} \quad (14)$$

DOI: 10.1021/acs.inorgchem.9b02096
Inorg. Chem. 2019, 58, 14507−14521

The predicted theoretical $\Delta_f H^{\ominus}(298.15\ \mathrm{K})$ is in the same range as the values reported in Table 9 and is in agreement with the new assessments of experimental data proposed here.

$PuO_2(OH)_2(g)$. Ebbinghaus' work reports the evaluation of the entropy and heat capacity of the plutonium oxy-hydroxide.[73] To compute the electronic contribution to the thermodynamics function of $PuO_2(OH)_2(g)$, Ebbinghaus also used, as for $PuO_3(g)$, the electronic spectrum of PuO_2^{2+}, but the main discrepancy in the standard entropy is due to the treatment of the vibrational frequencies. Actually, in Ebbinghaus' work a full analogy to $UO_2(OH)_2(g)$ was assumed, and the simulation treated the two torsional modes (for this molecule, internal rotations of OH groups) with the hindered rotor approach instead of harmonic oscillators. Nonetheless, in a recent study related to the thermodynamic properties of $UO_2(OH)_2(g)$,[80] no specific treatment has been made because it has been pointed out as an unreliable approach for these molecules in a previous review.[81] Therefore, similar behavior could be expected for $PuO_2(OH)_2(g)$ molecule: for reasons of computational cost, internal rotations are treated as other vibrations. Finally, for all these reasons, we prefer to rely on our calculations and we propose the following standard entropy of $PuO_2(OH)_2(g)$ at room temperature:

$$S^{\ominus}_{298K} = 355.74\ \mathrm{J\ K^{-1}\ mol^{-1}} \tag{15}$$

which is lower by 22.1 J K^{-1} mol^{-1} than Ebbinghaus' data (377.8 J K^{-1} mol^{-1}). The heat capacity function (in J K^{-1} mol^{-1}) is

$$C_p^{\ominus}(T) = 119.4872 + (3.3686 \times 10^{-2})(T/K) - (9.5789 \times 10^{-6})(T/K)^2 - (1.6030 \times 10^{6})(T/K)^{-2} \tag{16}$$

in the 298.15−1000 K range and

$$C_p^{\ominus}(T) = 134.27 + (1.5303 \times 10^{-2})(T/K) - (2.0559 \times 10^{-6})(T/K)^2 - (5.5254 \times 10^{6})(T/K)^{-2} \tag{17}$$

in the 1000−3000 K higher temperature range.

With respect to the standard heat of formation, the same drawbacks as for the PuO_3 molecule are pointed out regarding the experimental measurements carried out by Krikorian et al.[5] Additional issues may increase the uncertainty in this case, as the authors had to do some estimates related to water weighting in order to measure the steam pressure in the apparatus.[5] Thus, our calculations, which are not completely off from the reported experimental estimation (−1018.2 ± 3.3 kJ mol^{-1}),[5] can be considered as the most reliable ones. Our best estimate (SO-CASPT2) for the standard heat of formation thus is

$$\Delta_f H^{\ominus}(298.15\ \mathrm{K}) = -1012.6 \pm 38.0\ \mathrm{kJ\ mol^{-1}} \tag{18}$$

Thermodynamic Equilibrium Calculations. From an experimental viewpoint, the existence of $PuO_3(g)$ remains an open issue. The most recent analysis, involving mass spectrometric studies performed on the plutonium vapor phase in the Pu + O system, has not detected the PuO_3^+ vaporous species in the apparatus, whatever the vacuum or oxidative environment.[77] However, the authors concluded that dedicated experiments are needed to state the existence of this vapor species, especially due to the previous study by Ronchi where PuO_3 was briefly detected.[4]

To investigate the chemical equilibrium of the vapor phase over the plutonium oxygen phase with the current thermodynamic data, thermodynamic equilibrium computations were performed within the Nuclea Toolbox software[85] and the self-consistent MEPHISTA (version 17_1) database designed for nuclear fuel.[86] Isochoric calculations in which the oxygen amount is varying (associated with constant plutonium quantity) are made to show the plutonium vapor trend versus the oxygen potential. The simulation was run at 2270 K to reproduce the experiment under oxidative conditions, carried out by Gotcu-Freis et al.[77] Attention should be focused at the oxygen potential equal to about −130 kJ mol^{-1}, corresponding to the oxygen pressure of 100 Pa applied during the experiment. In order to perceive the effect of the newly determined thermodynamics functions, a first calculation with the original thermodynamic database (MEPHISTA-17_1) was performed (Figure 4a). At an oxygen potential of −130 kJ mol^{-1} the gaseous phase is mainly composed of PuO_2, though its partial pressure remains low. In addition, the contribution to the gaseous phase of PuO increases as the oxygen's chemical potential decreases.

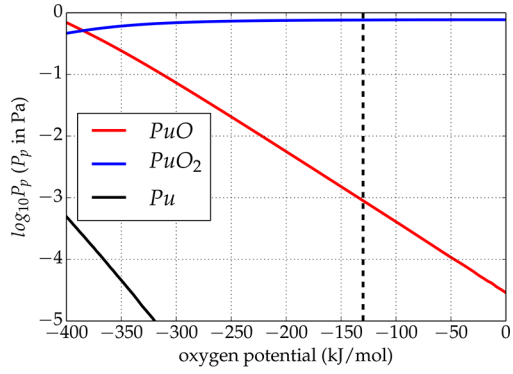

(a) MEPHISTA-17_1

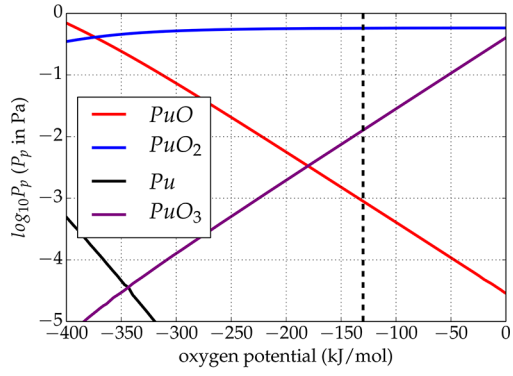

(b) Modified database

Figure 4. Thermodynamic equilibrium calculations: focus on the partial pressures of plutonium species at 2270 K versus the chemical potential of oxygen. The dashed line corresponds to an oxygen pressure of 100 Pa (−130 kJ mol^{-1}).

Conversely, with the updated database (Figure 4b), i.e. $PuO_3(g)$ is added and the Gibbs function of $PuO_2(g)$ is modified according to the present work. Unlike the first

DOI: 10.1021/acs.inorgchem.9b02096
Inorg. Chem. 2019, 58, 14507−14521

simulation, PuO_3 appears in the gaseous phase up to low oxygen potentials, whereas its partial pressure is higher than that of PuO for an oxygen potential of about −130 kJ mol^{-1}. This appears to contradict the analysis of Gotcu-Freis et al.,[77] in which PuO is detected whereas the same is not true for PuO_3. The dissociation energy of PuO_3 to PuO_2^+ is 1032 kJ mol^{-1}, calculated from the reviewed data of the ionization energy of PuO_2 (7.07 eV). The SO-CASPT2 calculations allow us to propose the value of 9.2 eV (887.5 kJ mol^{-1}) for the adiabatic ionization energy for PuO_3, about 0.9 eV lower that that predicted (10.1 eV) by scalar relativistic DFT calculations.[87] The PuO_3 ionization energy is just below the dissociation energy and therefore suggests that the fragmentation of PuO_3 to PuO_2^+ could be an important process and explains why PuO_3 is not detected. Finally, even if the temperature is high, these simulations show that the total partial pressure of plutonium remains rather low, whatever the database. At high oxygen potentials, a temperature drop should promote the plutonium trioxide over the dioxide with nevertheless a partial pressure lower than that obtained at 2270 K.

To extend the investigation to an oxygen/steam environment case, thermodynamic equilibrium calculations were also done under isobaric condition (standard pressure) with a constant amount of oxygen while a variable hydrogen inventory was used in order to shift the oxygen potential. The partial pressures of gaseous plutonium species versus the oxygen potential were calculated at the lowest possible temperature (1500 K) at which gaseous plutonium is present and in accordance with the simulation temperature used in the experiments dedicated to Pu(VI) volatility performed by Krikorian et al.[5] and Hubener et al.[6] At this temperature, the plutonium volatility is very low: i.e., $<10^{-11}$ bar whatever the oxygen potential. Under a purely oxygen atmosphere, as expected, only PuO_3 appears, but if steam is present, the $PuO_2(OH)_2$ species exists and rapidly becomes the main gaseous species when the steam fraction rises (see Figure 5).

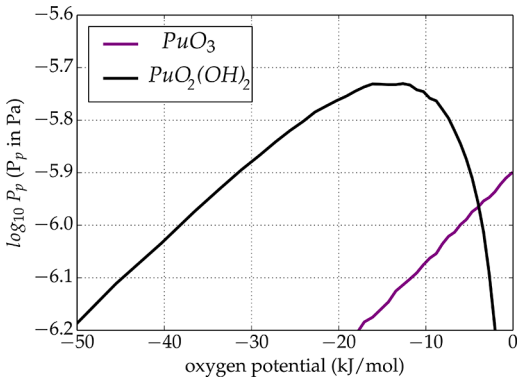

Figure 5. Focus on the partial pressures of plutonium species at 1500 K versus the chemical potential of oxygen under standard pressure conditions for the Pu−O−H system.

CONCLUSIONS

In conclusion, this work proposes a complete revision of the thermodynamics functions of the main gaseous species of the Pu−O−H system, namely PuO_2, PuO_3, and $PuO_2(OH)_2$, using accurate relativistic correlated quantum chemical calculations extrapolated to the complete basis set limit. This updated database is helpful to predict the most important thermophysical properties for nuclear safety and risk analysis: namely, the vapor pressure. Thermodynamic equilibrium calculations with the updated database performed at high temperature disclose new aspects of the volatility of plutonium under accidental conditions. They not only confirm the predominance of PuO_2 under an oxygen atmosphere but also validate the conjecture of Ronchi et al.[4] and Krikorian et al.[5] regarding the formation of the molecule $PuO_3(g)$ at high oxygen potentials. However, all reported quantum chemical calculations suggest that the stability of $PuO_3(g)$ might be hampered by fragmentation processes to lower-valent oxides. In the presence of steam, plutonium volatilizes into two competing Pu(VI) gaseous forms, $PuO_3(g)$, and $PuO_2(OH)_2(g)$, though their partial pressures are low: i.e., $<10^{-11}$ bar. This study increases the knowledge of the effective volatility of plutonium and calls for caution assessments and possibly new experiments in secured nuclear laboratories.

In addition to the nuclear implications, new insights into the electronic structure of the plutonium oxide and oxyhydroxide species have been gained, by confronting the results obtained with the two-component relativistic correlated $^2DC^M$-CCSD method and the more approximate two-step relativistic multireference method SO-CASPT2. Our SO-CASPT2 and $^2DC^M$-EOM-EE-CCSD results confirm the initial evidence by Feng and Peterson[41] that the ground state of PuO_2 is closed shell at the relativistic level with a $\Omega = 0_g^+$ character and provide compelling evidence that it is well separated by about several thousands of cm^{-1} from the first open-shell u state formally assigned as the PuO_2 ground state by La Macchia et al.[50] $^2DC^M$-EOM-IP-CCSD calculations place the adiabatic ionization energy of PuO_2 at 7.07 eV, in excellent agreement with the up to date experimental value. The electronic ground states of PuO_3 and $PuO_2(OH)_2$ exhibit strong multireference characters, and we evidence that multireference SO-CASPT2 is a quantitatively appropriate method to compute their enthalpies of formation. The reported values are in good agreement with the available data, making us confident about its predictive capability for other gas-phase heavy-element species with complex electronic structures.

ASSOCIATED CONTENT

Supporting Information

The Supporting Information is available free of charge on the ACS Publications website at DOI: 10.1021/acs.inorgchem.9b02096.

Mathematical formula used to compute the uncertainties, illustration of the ANO-RCC basis set convergence to the CBS limit, analysis of the spin-free and spin−orbit states of Pu, PuO_2, PuO_3, and $PuO_2(OH)_2$ and their SO-CASPT2 transition energies, up to 16000 cm^{-1}, molecular parameters and standard entropies of the $PuO_2(g)$, $PuO_3(g)$, and $PuO_2(OH)_2(g)$ molecules, heat capacity functions of the $PuO_2(g)$, $PuO_3(g)$, and $PuO_2(OH)_2(g)$ molecules, and atomization energies of PuO_2. The full data set is distributed through the Zenodo repository.[88] (PDF)

AUTHOR INFORMATION

Corresponding Author

*E-mail for V.V.: valerie.vallet@univ-lille.fr.

DOI: 10.1021/acs.inorgchem.9b02096
Inorg. Chem. 2019, 58, 14507−14521

ORCID

Florent Réal: 0000-0002-5163-1545
André Severo Pereira Gomes: 0000-0002-5437-2251
Valérie Vallet: 0000-0002-2202-3858

Notes

The authors declare no competing financial interest.

■ ACKNOWLEDGMENTS

We gratefully acknowledge financial support from the France-Canada Research Fund, Natural Sciences and Engineering Research Council of Canada (NSERC). This research was supported by the NEEDS environment project (TEMPO, "ThErmodynamique des Molécules de PlutOnium") funded in 2017. We acknowledge support by the French government through the Program "Investissement d'avenir" (LABEX CaPPA/ANR-11-LABX-0005-01 and I-SITE ULNE/ANR-16-IDEX-0004 ULNE), as well as by the Ministry of Higher Education and Research, Hauts de France council, and European Regional Development Fund (ERDF) through the Contrat de Projets Etat-Region (CPER CLIMIBIO). Furthermore, this work was granted access to the HPC resources of [CINES/IDRIS/TGCC] under the allocation 2016-2019 (x2016081859 and A0010801859, A0030801859, A0050800244) made by GENCI. We also acknowledge Małgorzata Olejniczak for her exploratory work on the benchmarking of relativistic DFT and MS-CASPT2 calculations. We further thank Sidi Souvi and Marc Barrachin for very fruitful discussions.

■ REFERENCES

(1) Šulka, M.; Cantrel, L.; Vallet, V. Theoretical Study of Plutonium(IV) Complexes Formed within the PUREX Process: A Proposal of a Plutonium Surrogate in Fire Conditions. *J. Phys. Chem. A* **2014**, *118*, 10073−10080.

(2) Konings, R. J. M.; Beneš, O.; Kovács, A.; Manara, D.; Sedmidubský, D.; Gorokhov, L.; Iorish, V. S.; Yungman, V.; Shenyavskaya, E.; Osina, E. The Thermodynamic Properties of the f-Elements and their Compounds. Part 2. The Lanthanide and Actinide Oxides. *J. Phys. Chem. Ref. Data* **2014**, *43*, 013101.

(3) Guéneau, C.; Chatillon, C.; Sundman, B. Thermodynamic modelling of the plutonium-oxygen system. *J. Nucl. Mater.* **2008**, *378*, 257−272.

(4) Ronchi, C.; Capone, F.; Colle, J. Y.; Hiernaut, J. P. Volatile molecule PuO_3 observed from subliming plutonium dioxide. *J. Nucl. Mater.* **2000**, *280*, 111−115.

(5) Krikorian, O.; Fontes, A.; Ebbinghaus, B.; Adamson, M. Transpiration studies on the volatilities of $PuO_3(g)$ and $PuO_2(OH)_2(g)$ from $PuO_2(s)$ in the presence of steam and oxygen and application to plutonium volatility in mixed-waste thermal oxidation processors. *J. Nucl. Mater.* **1997**, *247*, 161.

(6) Hübener, S.; Taut, S.; Vahle, A.; Bernhard, G.; Fanghänel, T. Thermochromatographic studies of plutonium oxides. *Radiochim. Acta* **2008**, *96*, 781−785.

(7) Sikkema, J.; Visscher, L.; Saue, T.; Ilias, M. The molecular mean-field approach for correlated relativistic calculations. *J. Chem. Phys.* **2009**, *131*, 124116.

(8) Infante, I.; Gomes, A. S. P.; Visscher, L. On the performance of the intermediate Hamiltonian Fock-space coupled-cluster method on linear triatomic molecules: The electronic spectra of NpO_2^+, NpO_2^{2+}, and PuO_2^{2+}. *J. Chem. Phys.* **2006**, *125*, 074301.

(9) Infante, I.; Eliav, E.; Vilkas, M. J.; Ishikawa, Y.; Kaldor, U.; Visscher, L. Fock space coupled cluster study on the electronic structure of the UO_2, UO_2^+, U^{4+}, and U^{5+} species. *J. Chem. Phys.* **2007**, *127*, 124308.

(10) Boguslawski, K.; Réal, F.; Tecmer, P.; Duperrouzel, C.; Gomes, A. S. P.; Legeza, Ö.; Ayers, P. W.; Vallet, V. On the Multi-Reference Nature of Plutonium Oxides: PuO_2^{2+}, PuO_2, PuO_3 and $PuO_2(OH)_2$. *Phys. Chem. Chem. Phys.* **2017**, *19*, 4317−4329.

(11) Kovács, A. Electronic structure and spectroscopic properties of mixed sodium actinide oxides Na_2AnO_4 (An = U, Np, Pu, Am). *J. Mol. Struct.* **2017**, *1132*, 95−101.

(12) Gomes, A. S. P.; Jacob, C. R.; Visscher, L. Calculation of local excitations in large systems by embedding wave-function theory in density-functional theory. *Phys. Chem. Chem. Phys.* **2008**, *10*, 5353−5362.

(13) Ruipérez, F.; Danilo, C.; Réal, F.; Flament, J.-P.; Vallet, V.; Wahlgren, U. *Ab initio* theoretical study of the electronic structure of UO_2^+ and $[UO_2(CO_3)_3]^{5-}$. *J. Phys. Chem. A* **2009**, *113*, 1420−1428.

(14) Weigand, A.; Cao, X.; Vallet, V.; Flament, J.-P.; Dolg, M. Multiconfiguration Dirac-Hartree-Fock Adjusted Energy-consistent Pseudopotential for Uranium: Spin-orbit Configuration Interaction and Fock-Space Coupled-Cluster Study of U^{4+} and U^{5+}. *J. Phys. Chem. A* **2009**, *113*, 11509−11516.

(15) Réal, F.; Gomes, A. S. P.; Visscher, L.; Vallet, V.; Eliav, E. Benchmarking Electronic Structure Calculations on the Bare UO_2^{2+} ion: How Different are Single and Multireference Electron Correlation Methods? *J. Phys. Chem. A* **2009**, *113*, 12504−12511.

(16) Tecmer, P.; Gomes, A. S. P.; Ekström, U.; Visscher, L. Electronic Spectroscopy of UO_2^{2+}, NUN and NUO^+. *Phys. Chem. Chem. Phys.* **2011**, *13*, 6249−6259.

(17) Tecmer, P.; van Lingen, H.; Gomes, A. S. P.; Visscher, L. The electronic spectrum of $CUONg_4$ (Ng = Ne, Ar, Kr, Xe): New insights in the interaction of the CUO molecule with noble gas matrices. *J. Chem. Phys.* **2012**, *137*, 084308.

(18) Gomes, A. S. P.; Jacob, C. R.; Réal, F.; Vallet, V.; Visscher, L. Towards systematically improvable models for actinides in condensed phase: the electronic spectrum of uranyl in $Cs_2UO_2Cl_4$ as a test case. *Phys. Chem. Chem. Phys.* **2013**, *15*, 15153−15162.

(19) Shee, A.; Saue, T.; Visscher, L.; Gomes, A. S. P. Equation-of-Motion Coupled-Cluster Theory based on the 4-component Dirac-Coulomb(-Gaunt) Hamiltonian. Energies for single electron detachment, attachment and electronically excited states. *J. Chem. Phys.* **2018**, *149*, 174113.

(20) Rauh, E. G.; Ackermann, R. J. First ionization potentials of some refractory oxide vapors. *J. Chem. Phys.* **1974**, *60*, 1396−1400. Rauh, E. G.; Ackermann, R. Erratum: First ionization potentials of some refractory oxide vapors. *J. Chem. Phys.* **1974**, *64*, 1862.

(21) Capone, F.; Colle, Y.; Hiernaut, J. P.; Ronchi, C. Mass Spectrometric Measurement Of the Ionization Energies and Cross Sections Of Uranium and Plutonium Oxide Vapors. *J. Phys. Chem. A* **1999**, *103*, 10899−10906.

(22) Santos, M.; Marçalo, J.; Pires de Matos, A.; Gibson, J. K.; Haire, R. G. Gas-Phase Oxidation Reactions of Neptunium and Plutonium Ions Investigated via Fourier Transform Ion Cyclotron Resonance Mass Spectrometry. *J. Phys. Chem. A* **2002**, *106*, 7190−7194.

(23) Ruscic, B.; Bross, D. H. *Active Thermochemical Tables (ATcT) values based on ver. 1.122e of the Thermochemical Network*; Argonne National Laboratory (2019); available at ATcT.anl.gov. 2019; https://atct.anl.gov/.

(24) Lemire, R. J.; Fuger, J.; Nitsche, H.; Potter, P.; Rand, M. H.; Rydberg, J.; Spahiu, K.; Sullivan, J. A.; Ullman, W. J.; Vitorge, P.; Wanner, H. In *Chemical Thermodynamics of Neptunium and Plutonium*; OECD Nuclear Energy Agency, Ed.; Elsevier: 2001; Chemical thermodynamics.

(25) Küchle, W.; Dolg, M.; Stoll, H.; Preuss, H. Energy-adjusted pseudopotentials for the actinides. Parameter sets and test calculations for thorium and thorium monoxide. *J. Chem. Phys.* **1994**, *100*, 7535−7542.

(26) Cao, X.; Dolg, M.; Stoll, H. Valence basis sets for relativistic energy-consistent small-core actinide pseudopotentials. *J. Chem. Phys.* **2003**, *118*, 487−496.

DOI: 10.1021/acs.inorgchem.9b02096
Inorg. Chem. 2019, 58, 14507−14521

(27) Dunning, T. H., Jr. Gaussian basis sets for use in correlated molecular calculations. I. The atoms boron through neon and hydrogen. *J. Chem. Phys.* **1989**, *90*, 1007−1023.
(28) Becke, A. D. Density-functional thermochemistry. III. The role of exact exchange. *J. Chem. Phys.* **1993**, *98*, 5648−5652.
(29) Frisch, M. J. et al. *Gaussian 09, Revision C.02*; Gaussian, Inc.: Wallingford, CT, 2004.
(30) Barone, V. Vibrational zero-point energies and thermodynamic functions beyond the harmonic approximation. *J. Chem. Phys.* **2004**, *120*, 3059−3065.
(31) Barone, V. Anharmonic vibrational properties by a fully automated second-order perturbative approach. *J. Chem. Phys.* **2005**, *122*, 014108.
(32) Roos, B. O.; Lindh, R.; Malmqvist, P.-Å.; Veryazov, V.; Widmark, P.-O. Main group atoms and dimers studied with a new relativistic ANO basis set. *J. Phys. Chem. A* **2004**, *108*, 2851−2858.
(33) Roos, B. O.; Lindh, R.; Malmqvist, P.-Å.; Veryazov, V.; Widmark, P.-O. New relativistic ANO basis sets for actinide atoms. *Chem. Phys. Lett.* **2005**, *409*, 295−299.
(34) Karton, A.; Martin, J. M. L. Comment on: "Estimating the Hartree-Fock limit from finite basis set calculations" [Jensen F (2005) Theor Chem Acc 113:267]. *Theor. Chem. Acc.* **2006**, *115*, 330−333.
(35) Feller, D.; Peterson, K. A.; Dixon, D. A. A survey of factors contributing to accurate theoretical predictions of atomization energies and molecular structures. *J. Chem. Phys.* **2008**, *129*, 204105.
(36) Feller, D.; Peterson, K. A.; Grant Hill, J. On the effectiveness of CCSD(T) complete basis set extrapolations for atomization energies. *J. Chem. Phys.* **2011**, *135*, 044102.
(37) Lu, Q.; Peterson, K. A. Correlation consistent basis sets for lanthanides: The atoms La-Lu. *J. Chem. Phys.* **2016**, *145*, 054111.
(38) Watts, J. D.; Gauss, J.; Bartlett, R. J. Coupled-cluster methods with noniterative triple excitations for restricted open-shell Hartree-Fock and other general single determinant reference functions. Energies and analytical gradients. *J. Chem. Phys.* **1993**, *98*, 8718−8733.
(39) Werner, H.-J. et al. *MOLPRO, Version 2015.1, A Package Of Ab Initio Programs*; 2015; see http://www.molpro.net.
(40) Bross, D. H.; Peterson, K. A. Composite thermochemistry of gas phase U(VI)-containing molecules. *J. Chem. Phys.* **2014**, *141*, 244308.
(41) Feng, R.; Vasiliu, M.; Peterson, K. A.; Dixon, D. A. Acidity of $M(VI)O_2(OH)_2$ for M = Group 6, 16, and U as Central Atoms. *J. Phys. Chem. A* **2017**, *121*, 1041−1050.
(42) Gagliardi, L.; Roos, B. O. Multiconfigurational quantum chemical methods for molecular systems containing actinides. *Chem. Soc. Rev.* **2007**, *36*, 893−903.
(43) Knowles, P. J.; Werner, H.-J. An efficient second-order MC-SCF method for long configuration expansions. *Chem. Phys. Lett.* **1985**, *115*, 259−267.
(44) Werner, H.-J.; Knowles, P. J. A Second Order Multi-configuration SCF Procedure with Optimum Convergence. *J. Chem. Phys.* **1985**, *82*, 5053−5063.
(45) Bovey, L.; Gerstenkorn, S. Ground State of the First Spectrum of Plutonium (Pu i), from an Analysis of Its Atomic Spectrum. *J. Opt. Soc. Am.* **1961**, *51*, 522−525.
(46) Blaise, J.; Fred, M.; Gerstenkorn, S.; Judd, B. Multiplet fondamental du spectre daarc du plutonium. *C.R. Acad. Sci., Fr.* **1962**, *255*, 2403−2405.
(47) Blaise, J.; Wyart, J.; Conway, J.; Worden, E. Generalized Parametric Study of $5f^N$ and $5f^N7s$ Configurations. *Phys. Scr.* **1980**, *22*, 224−230.
(48) Malmqvist, P.-Å.; Rendell, A.; Roos, B. O. The restricted active space self-consistent-field method, implemented with a split graph unitary group approach. *J. Phys. Chem.* **1990**, *94*, 5477−5482.
(49) Denning, R. G. Electronic structure and bonding in actinyl ions and their analogs. *J. Phys. Chem. A* **2007**, *111*, 4125−4143.
(50) La Macchia, G.; Infante, I.; Raab, J.; Gibson, J. K.; Gagliardi, L. A theoretical study of the ground state and lowest excited states of $PuO^{0/+/+2}$ and $PuO_2^{0/+/+2}$. *Phys. Chem. Chem. Phys.* **2008**, *10*, 7278−7283.
(51) Stalring, J.; Bernhardsson, A.; Lindh, R. Analytical gradients of a state average MCSCF state and a state average diagnostic. *Mol. Phys.* **2001**, *99*, 103−114.
(52) Finley, J.; Malmqvist, P.-Å.; Roos, B. O.; Serrano-Andrés, L. The multi-state CASPT2 method. *Chem. Phys. Lett.* **1998**, *288*, 299−306.
(53) Forsberg, N.; Malmqvist, P. Å. Multiconfiguration perturbation theory with imaginary level shift. *Chem. Phys. Lett.* **1997**, *274*, 196−204.
(54) Ghigo, G.; Roos, B. O.; Malmqvist, P.-Å. A modified definition of the zeroth order Hamiltonian in multii-configurational perturbation theory (CASPT2). *Chem. Phys. Lett.* **2004**, *396*, 142−149.
(55) Malmqvist, P. Å.; Roos, B. O.; Schimmelpfennig, B. The restricted active space (RAS) state interaction approach with spin-orbit coupling. *Chem. Phys. Lett.* **2002**, *357*, 230−240.
(56) Heß, B. A.; Marian, C. M.; Wahlgren, U.; Gropen, O. A mean-field spin-orbit method applicable to correlated wavefunctions. *Chem. Phys. Lett.* **1996**, *251*, 365−371.
(57) Schimmelpfennig, B. *AMFI, an Atomic Mean-Field Integral program*, 1996.
(58) Francesco, A.; et al. Molcas 8: New capabilities for multiconfigurational quantum chemical calculations across the periodic table. *J. Comput. Chem.* **2015**, *37*, 506−541.
(59) Visscher, L.; Lee, T. J.; Dyall, K. G. Formulation and implementation of a relativistic unrestricted coupled-cluster method including noniterative connected triples. *J. Chem. Phys.* **1996**, *105*, 8769−8776.
(60) Visscher, L.; Eliav, E.; Kaldor, U. Formulation and implementation of the relativistic Fock-space coupled cluster method for molecules. *J. Chem. Phys.* **2001**, *115*, 9720−9726.
(61) DIRAC, a relativistic ab initio electronic structure program, Release DIRAC18 (2018), written by Saue, T.; Visscher, L.; Jensen, H. J. Aa.; Bast, R., with contributions from V. Bakken, K. G. Dyall, S. Dubillard, U. Ekström, E. Eliav, T. Enevoldsen, E. Faßhauer, T. Fleig, O. Fossgaard, A. S. P. Gomes, E. D. Hedegård, T. Helgaker, J. Henriksson, M. Iliaš, Ch. R. Jacob, S. Knecht, S. Komorovský, O. Kullie, J. K. Lærdahl, C. V. Larsen, Y. S. Lee, H. S. Nataraj, M. K. Nayak, P. Norman, G. Olejniczak, J. Olsen, J. M. H. Olsen, Y. C. Park, J. K. Pedersen, M. Pernpointner, R. di Remigio, K. Ruud, P. Sałek, B. Schimmelpfennig, A. Shee, J. Sikkema, A. J. Thorvaldsen, J. Thyssen, J. van Stralen, S. Villaume, O. Visser, T. Winther, and S. Yamamoto (available at DOI: 10.5281/zenodo.2253986, see also http://www.diracprogram.org).
(62) Dyall, K. G. Relativistic double-zeta, triple-zeta, and quadruple-zeta basis sets for the 7*p* elements, with atomic and molecular applications. *Theor. Chem. Acc.* **2012**, *131*, 1172.
(63) Dyall, K. G. Relativistic double-zeta, triple-zeta, and quadruple-zeta basis sets for the actinides Ac Lr. *Theor. Chem. Acc.* **2007**, *117*, 491−500.
(64) Visscher, L. Approximate molecular relativistic Dirac-Coulomb calculations using a simple Coulombic correction. *Theor. Chem. Acc.* **1997**, *98*, 68−70.
(65) Thyssen, J. Development and Applications of Methods for Correlated Relativistic Calculations of Molecular Properties. Ph.D. thesis, University of Southern Denmark, 2001.
(66) Kovács, A. Relativistic Multireference Quantum Chemical Study of the Electronic Structure of Actinide Trioxide Molecules. *J. Phys. Chem. A* **2017**, *121*, 2523−2530.
(67) Feng, R.; Peterson, K. A. Correlation consistent basis sets for actinides. II. The atoms Ac and Np−Lr. *J. Chem. Phys.* **2017**, *147*, 084108.
(68) Infante, I.; Kovacs, A.; La Macchia, G.; Moughal Shahi, A. R.; Gibson, J. K.; Gagliardi, L. Ionization Energies for the Actinide Mono- and Dioxides Series, from Th to Cm: Theory versus Experiment. *J. Phys. Chem. A* **2010**, *114*, 6007−6015.
(69) Archibong, E. F.; Ray, A. K. An ab initio study of PuO_2 and of PuN_2. *J. Mol. Struct.: THEOCHEM* **2000**, *530*, 165−170.

DOI: 10.1021/acs.inorgchem.9b02096
Inorg. Chem. 2019, 58, 14507−14521

(70) Batista, E. R.; Martin, R. L.; Hay, P. J.; Peralta, J. E.; Scuseria, G. E. Density functional investigations of the properties and thermochemistry of UF_6 and UF_5 using valence-electron and all-electron approaches. *J. Chem. Phys.* **2004**, *121*, 2144−2150.
(71) Capone, F.; Colle, J. Y.; Hiernaut, J. P.; Ronchi, C. Controversy on the First Ionization Potential of PuO_2 (Nearly) Settled by New Experimental Evidence. *J. Phys. Chem. A* **2005**, *109*, 12054−12058.
(72) Gibson, J. K.; Santos, M.; Marçalo, J.; Leal, J. P.; Pires de Matos, A.; Haire, R. G. Comment on "Controversy on the First Ionization Potential of PuO_2 (Nearly) Settled by New Experimental Evidence. *J. Phys. Chem. A* **2006**, *110*, 4131−4132.
(73) Ebbinghaus, B. B. *Calculated thermodynamic functions for gas phase uranium, neptunium, plutonium and americium oxides (AnO_3), oxyhydroxides ($AnO_2(OH)_2$)), oxychlorides (AnO_2Cl_2) and oxyfluorides (AnO_2F_2)*; **2002**; DOI: 10.2172/15002515.
(74) Green, D. W.; Reedy, G. T. Infrared spectra of matrix isolated plutonium oxides. *J. Chem. Phys.* **1978**, *69*, 544.
(75) Kovács, A.; Konings, R. J. M.; Gibson, J. K.; Infante, I.; Gagliardi, L. Quantum Chemical Calculations and Experimental Investigations of Molecular Actinide Oxides. *Chem. Rev.* **2015**, *115*, 1725−1759.
(76) Miradji, F.; Souvi, S.; Cantrel, L.; Louis, F.; Vallet, V. Thermodynamic Properties of Gaseous Ruthenium Species. *J. Phys. Chem. A* **2015**, *119*, 4961−4971.
(77) Gotcu-Freis, P.; Colle, J.-Y.; Hiernaut, J.-P.; Naisse, F.; Guéneau, C.; Konings, R. Mass spectrometric studies of the vapour phase in the (Pu.O) system. *J. Chem. Thermodyn.* **2011**, *43*, 1164−1173.
(78) Eisenstein, J. C.; Pryce, M. H. L. Interpretation of the Solution Absorption Spectra of the $(PuO_2)^{+2}$ and $(NpO_2)_+$. *J. Res. Natl. Bur. Stand., Sect. A* **1966**, *70A*, 165−173.
(79) Krikorian, O. H.; Ebbinghaus, B. B.; Adamson, M. G.; Fontes, J. A. S.; Fleming, D. L. *Experimental Studies and Themordynamic Modeling of Volatilities of Uranium, Plutonium, and Americium from Their Oxides and from Their Oxides Interacted with Ash*; Report UCRL-ID-114774, 1993; DOI: 10.2172/10190948.
(80) Konings, R.; Kovács, A.; Beneš, O. The thermodynamic properties of gaseous $UO_2(OH)_2$. *J. Nucl. Mater.* **2017**, *496*, 163−165.
(81) Guillaumont, R.; Fanghänel, T.; Neck, V.; Fuger, J.; Palmer, D. A.; Grenthe, I.; Rand, M. H. *Update on the chemical thermodynamics of uranium, neptunium, plutonium, americium and technetium*; 2003.
(82) Ruscic, B.; Boggs, J. E.; Burcat, A.; Császár, A. G.; Demaison, J.; Janoschek, R.; Martin, J. M. L.; Morton, M. L.; Rossi, M. J.; Stanton, J. F.; et al. IUPAC Critical Evaluation of Thermochemical Properties of Selected Radicals. Part I. *J. Phys. Chem. Ref. Data* **2005**, *34*, 573−656.
(83) Cordfunke, E. H. P.; Konings, R. J. M. Thermochemical data for reactor materials and fission products: The ECN database. *J. Phase Equilib.* **1993**, *14*, 457−464.
(84) Glushko, V.; Gurvich, L.; Veits, I.; Medvedev, V.; Khachkuruzov, G.; Yungman, V.; Bergman, G. In *Thermodynamic Properties of Individual Substances*; Hemisphere: 1978−1982; Vol. *1*−*4*.
(85) Piar, B. *NucleaToolbox 2.3.0*; IRSN.
(86) Cheynet, B.; Fischer, E. *MEPHISTA: A thermodynamic database for new generation nuclear fuels*; unpublished, 2007.
(87) Gao, T.; Zhu, Z.-H.; Wang, X.-L.; Sun, Y.; Meng, D.-Q. Molecular structures and molecular spectra for PuO_3 and PuO_3^+. *Acta Chim* **2004**, *62*, 454−460.
(88) Kervazo, S.; Réal, F.; Virot, F.; Gomes, A. S. P.; Vallet, V. *Accurate Predictions of Volatile Plutonium Thermodynamic Properties*. Zenodo http://dx.doi.org/10.5281/zenodo.3380352, 2019.

DOI: 10.1021/acs.inorgchem.9b02096
Inorg. Chem. 2019, 58, 14507−14521